AD-A181 747 THE EFFECTS OF DOPPLER SHIFTING ON THE FREQUENCY SPECTRA OF ATMOSPHERIC G..(U) NATIONAL OCEANIC AND ATMOSPHERIC ADMINISTRATION BOULDER CO T E VAN ZANDT ET AL. JAN 87

1/1

UNCLASSIFIED F/G 4/1 NL

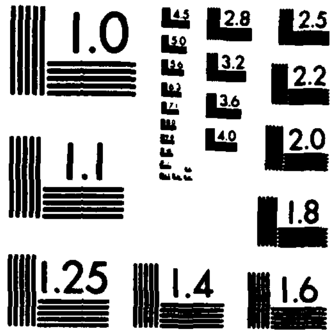

MICROCOPY RESOLUTION TEST CHART
NATIONAL BUREAU OF STANDARDS-1963-A

DTIC FILE COPY

AD-A181 747

AFOSR-TR- 87-0624

THE EFFECTS OF DOPPLER SHIFTING ON THE FREQUENCY SPECTRA OF ATMOSPHERIC GRAVITY WAVES

FINAL REPORT

AFOSR-ISSA-86-0050
AFOSR-ISSA-87-0080

Thomas E. Van Zandt
National Oceanic and Atmospheric Administration

David C. Fritts
Geophysical Institute, University of Alaska

January 1987

87 5 20 142

Unclassified

SECURITY CLASSIFICATION OF THIS PAGE

AD-A181 747

REPORT DOCUMENTATION PAGE

1a. REPORT SECURITY CLASSIFICATION Unclassified	1b. RESTRICTIVE MARKINGS
2a. SECURITY CLASSIFICATION AUTHORITY	3. DISTRIBUTION/AVAILABILITY OF REPORT Approved for public release; distribution unlimited
2b. DECLASSIFICATION/DOWNGRADING SCHEDULE	
4. PERFORMING ORGANIZATION REPORT NUMBER(S)	5. MONITORING ORGANIZATION REPORT NUMBER(S) AFOSR-TR- 87-0624
6a. NAME OF PERFORMING ORGANIZATION National Oceanic & Atmospheric 6b. OFFICE SYMBOL (If applicable) Admin	7a. NAME OF MONITORING ORGANIZATION AFOSR/NC
6c. ADDRESS (City, State and ZIP Code) 325 Broadway Boulder CO 80303	7b. ADDRESS (City, State and ZIP Code) Bldg 410 Bolling AFB DC 20332-6448
8a. NAME OF FUNDING/SPONSORING ORGANIZATION AFOSR 8b. OFFICE SYMBOL (If applicable) NC	9. PROCUREMENT INSTRUMENT IDENTIFICATION NUMBER AFOSR-ISSA-86-0050 AFOSR-ISSA-87-0080
8c. ADDRESS (City, State and ZIP Code) Bldg 410 Bolling AFB DC 20332-6448	10. SOURCE OF FUNDING NOS. PROGRAM ELEMENT NO.: 61102F PROJECT NO.: 2310 TASK NO.: A1 WORK UNIT NO.:

11. TITLE (Include Security Classification) The Effects of Doppler Shifting on the Frequency Spectra of Atmospheric Gravity Waves (U)

12. PERSONAL AUTHOR(S)
Thomas E. Van Zandt and David C. Fritts

13a. TYPE OF REPORT	13b. TIME COVERED	14. DATE OF REPORT (Yr., Mo., Day)	15. PAGE COUNT
Final Report	FROM ______ TO ______	87 January	53

16. SUPPLEMENTARY NOTATION

17. COSATI CODES		
FIELD	GROUP	SUB. GR.

18. SUBJECT TERMS (Continue on reverse if necessary and identify by block number)
anistrophy MU radar irregularities
gravity wave dissipation

19. ABSTRACT (Continue on reverse if necessary and identify by block number)

Spectra of atmospheric motions as a function of observed frequency may depart significantly from the spectra as a function of intrinsic frequency due to a nonzero mean wind. In this paper, we examine the effects of Doppler shifting on a model spectrum of atmospheric gravity waves. In order to gain insight into the effects of Doppler shifting, we have derived analytic solutions by approximation of the intrinsic frequency spectra and the gravity wave dispersion relation. Our results reveal that Doppler shifting can have major effects on the observed frequency spectrum of both horizontal and vertical gravity wave energy. For levels of Doppler shifting representative of the lower and middle atmosphere, possible effects include a substantial enhancement of horizontal energy density at higher observed frequencies, a corresponding reduction of the vertical energy density at higher frequencies above the buoyancy frequency. The predicted effects are found to be consistent with some of the features of the observed frequency spectra.

20. DISTRIBUTION/AVAILABILITY OF ABSTRACT UNCLASSIFIED/UNLIMITED ☒ SAME AS RPT. ☒ DTIC USERS ☐	21. ABSTRACT SECURITY CLASSIFICATION Unclassified
22a. NAME OF RESPONSIBLE INDIVIDUAL Lt Col James P. Koermer	22b. TELEPHONE NUMBER (Include Area Code) (202) 767-4960 22c. OFFICE SYMBOL NC

DD FORM 1473, 83 APR EDITION OF 1 JAN 73 IS OBSOLETE.

87 5 20 112

UNCLASSIFIED

SECURITY CLASSIFICATION OF THIS PAGE

Abstract

Spectra of atmospheric motions as a function of observed frequency may depart significantly from the spectra as a function of intrinsic frequency due to a nonzero mean wind. In this paper ~~we~~ examines the effects of Doppler shifting on a model spectrum of atmospheric gravity waves. ~~In order~~ to gain insight into the effects of Doppler shifting, we ~~have~~ derived analytic solutions by approximation of the intrinsic frequency spectra and the gravity wave dispersion relation. Our results reveal that Doppler shifting can have major effects on the observed frequency spectrum of both horizontal and vertical gravity wave energy. For levels of Doppler shifting representative of the lower and middle atmosphere, possible effects include a substantial enhancement of horizontal energy density at higher observed frequencies, a corresponding reduction of the vertical energy density at higher frequencies, and a significant transfer of vertical energy to observed frequencies above the buoyancy frequency. The predicted effects are found to be consistent with some of the features of the observed frequency spectra.

Keywords: Anisotropy

1. INTRODUCTION

Internal gravity waves are known to contribute significantly to the atmospheric fluctuation spectrum at a range of scales and frequencies. In addition, they are now understood to have a number of important effects in the lower and middle atmosphere. Foremost among these, and the subjects of many recent studies, are the induced drag and turbulent diffusion arising from the saturation of upward propagating gravity waves in the middle atmosphere (see Fritts, 1984, for a review). More recent studies suggest that saturation processes may also be important in the lower atmosphere. Palmer et al. (1986) have suggested that gravity wave drag may be required to account for the mean structure of the tropospheric jet. At the same time, Smith et al. (1987) have provided evidence that part of the gravity wave spectrum may be saturated throughout the atmosphere, implying a possibility of induced drag and diffusion at all heights.

The importance of gravity waves, both in accounting for a significant portion of the atmospheric motion spectrum and in driving the large-scale circulation and thermal structure of the lower and middle atmosphere has stimulated a number of studies of the dominant gravity wave scales, characteristics, and effects. Some of these have focussed on the determination of individual wave parameters (Smith and Fritts, 1983; Meek et

al., 1985a) or saturation processes (Fritts and Rastogi, 1985), while others have addressed gravity wave climatologies and effects in a statistical manner (Vincent and Reid, 1983; Smith et al., 1985; Meek et al., 1985b; Fukao et al., 1985; Vincent and Fritts, 1987; Fritts and Vincent, 1987). While the former studies are needed to understand the detailed processes by which gravity waves propagate, dissipate, and contribute to drag and diffusion, statistical studies are essential in order to understand the average, integrated effects of gravity waves in the lower and middle atmosphere and to parameterize these effects in global circulation models. Thus it is important to understand any effects that may complicate or limit the interpretation of gravity wave spectra.

A prime example of such a complication of the spectral approach is the Doppler shifting of gravity wave frequencies due to a nonzero mean wind. While the effects of Doppler shifting should not cause difficulties in case studies of gravity wave motions and effects, they pose serious problems for spectral studies. Indeed, neglect of the effects of Doppler shifting may have lead to erroneous inferences concerning the nature of the motion spectrum (Gage and Nastrom, 1985).

VanZandt (1982) proposed that the small-scale fluctuations of wind in the lower atmosphere can be described

by a model spectrum of gravity wave motions very similar to the Garrett and Munk (1972, 1975) model that has been so successful in describing the corresponding fluctuations in the ocean. The model spectrum is formulated in terms of wavenumber and frequency, with the spectral shapes chosen to fit the observations as well as possible, while remaining consistent with the gravity wave dispersion relation. Thus, the model was rather empirical. Recent studies of the saturation of gravity wave spectra have removed some of the empiricism by providing theoretical support for the shape of the vertical wavenumber spectrum.

There remained, however, a major difficulty in applying the existing model to atmospheric frequency spectra because of its dependence on intrinsic frequency, i.e., the frequency measured with respect to the local mean flow. Unlike the ocean, where the observed frequencies are very nearly equal to the intrinsic frequencies because the mean current is usually much smaller than the intrinsic phase speeds of the dominant gravity waves, the mean wind in the atmosphere is often larger than the intrinsic phase speeds. When this happens, Doppler-shifting effects can be substantial and the intrinsic frequency spectra cannot be expected to apply.

With the above discussion in mind, the primary goals of the present study are 1) to emphasize the role of Doppler

shifting in altering the observed frequency spectra due to gravity wave motions and 2) to show that the changes arising as a result of Doppler shifting can account for some of the observed features of the atmospheric frequency spectra. To facilitate our discussion of the physics of Doppler shifting and provide a discussion that is easy to follow, we employ approximations to the observed motion spectra and the gravity wave dispersion relation that permit us to obtain analytic results. We believe this offers significant advantages over the treatment of Doppler shifting by Scheffler and Liu (1985, 1986), which is more accurate and complete, but less intuitive and illustrative. We begin in Section 2 with a discrete intrinsic frequency spectrum in order to illustrate the manner in which both discrete and continuous wavenumber spectra are affected by Doppler shifting. The resulting frequency spectrum is seen to depend fundamentally on the distribution of energy with horizontal wavenumber (or phase speed). In Section 3, we introduce a continuous intrinsic frequency spectrum. The shapes and variability with anisotropy and degree of Doppler shifting are examined in detail in Section 4. It is shown that realistic magnitudes of the mean wind can cause the shapes of the observed spectra to be quite different from the intrinsic spectra and that the spectral changes implied by Doppler shifting are consistent with some of the observed features of

the frequency spectra. The conclusions of this study are presented in Section 5.

2. DOPPLER SHIFTING OF DISCRETE INTRINSIC FREQUENCY SPECTRA

The purpose of this section is to demonstrate the effects of Doppler shifting on a discrete intrinsic frequency spectrum for both discrete and continuous horizontal wavenumber spectra. This will provide a basis for understanding the effects of Doppler shifting on more realistic spectra, which are treated in the following sections.

We first consider the normalized energy spectrum corresponding to a monochromatic wave motion at intrinsic frequency $\omega' = \omega_o'$ and horizontal wavenumber $\mathbf{k} = \mathbf{k}_o$. This is given by

$$E(\mathbf{k},\omega') = \delta(\mathbf{k}-\mathbf{k}_o)\delta(\omega'-\omega_o'), \qquad (1)$$

where the δ's are Dirac delta functions. The consequences of Doppler shifting of this simple spectrum are, of course, trivial. If the wave motion occurs in an environment with a mean wind $\bar{\mathbf{u}}$ normal to the horizontal intrinsic phase velocity of the wave, of magnitude $\mathbf{c}_o' = \mathbf{k}_o\omega_o'/k_o^2$, the frequency seen by an observer at rest remains unaltered. However, if the mean motion has a component in the direction of wave propagation, the observed (Doppler-shifted) frequency is given by

$$\omega = \omega' + \mathbf{k}\cdot\bar{\mathbf{u}} = \omega_o' + k_o\bar{u}\cos\phi$$

$$= \omega_o'(1 + \bar{u}\cos\phi/c_o')$$

$$= \omega_o'(1 + \beta_o\cos\phi), \qquad (2)$$

where k_o is the (positive) magnitude of $\mathbf{k}$, ϕ is the angle between the horizontal components of $\mathbf{k}$ and $\bar{\mathbf{u}}$ and $\beta_o = \bar{u}/c_o'$ is the scaled mean wind. The fractional frequency shift is given by

$$\frac{\omega - \omega_o'}{\omega_o'} = \beta_o\cos\phi \qquad (3)$$

The quantity $\beta_o\cos\phi$ thus provides a convenient measure of the effects of Doppler shifting on the frequency spectra of observed wave motions. It is generalized below to a spectrum of waves.

In the case of equal and opposite wave motions at intrinsic frequency ω_o' and with horizontal wavenumbers $\mathbf{k}_o$ and $-\mathbf{k}_o$, Doppler shifting results in two observed frequencies up- and down-shifted from the intrinsic frequency by equal amounts. For a more general gravity wave spectrum with a range of horizontal wavenumbers and directions of propagation, energy can be Doppler shifted to a broad range of observed frequencies above and below the intrinsic frequency, as shown below.

We now consider a superposition of waves all with the same intrinsic frequency ω_o', but with a continuum of horizontal wavenumbers, with an energy density given by

$$E(k,\omega') = \frac{\delta(\omega'-\omega_o')x^a}{(1 + x)^{t+a}}, \qquad (4)$$

where $x = k/k_*$ and a, t, and k_* are parameters that must be chosen to fit the observed spectra, subject to certain constraints. Indeed, Garrett and Munk (1975) and VanZandt (1982) fitted the observed oceanic and atmospheric spectra, respectively, with $a = 0$ and $t = 2.4 - 2.5$. At sufficiently small x, the logarithmic slope of E is a, and at sufficiently large x, it is -t. The slope changes from a to -t near $k = k_*$. Moreover, with reasonable values of a and t, most of the energy in the spectrum lies within a factor of three of k_*. Thus, k_* plays a critical role in the description of the spectrum. For this reason, we have chosen to call k_* the "characteristic horizontal wavenumber". It is, of course, the same as the "horizontal wavenumber bandwidth" of Garrett and Munk (1975).

In order to obtain the energy distribution as a function of observed frequency, we must express k/k_* in terms of intrinsic and observed frequencies. From (2)

$$k = (\omega - \omega')/\bar{u} \cos\phi. \qquad (5)$$

The gravity wave dispersion relation for hydrostatic, two-dimensional motions with $f^2 << \omega^2 << N^2$ is $k = \omega' m/N$, where f and N are the inertial and the buoyancy (Brunt-Vaisala) frequencies, respectively, and m is the vertical wavenumber. Then the characteristic horizontal wavenumber k_* can be related to ω' and the characteristic vertical wavenumber m_*, which Garrett and Munk (1975) and VanZandt (1982) assume is independent of ω', by

$$k_* = \frac{\omega' m_*}{N}. \tag{6}$$

Then

$$\frac{k}{k_*} = \frac{\omega-\omega'}{\bar{u}\cos\phi}\,\frac{N}{\omega' m_*} = \frac{\omega-\omega'}{\omega'}\,\frac{c_*'}{\bar{u}\cos\phi} = \frac{\omega-\omega'}{\omega'}\,\frac{1}{\beta\cos\phi}, \tag{7}$$

where c_*' is the characteristic intrinsic horizontal phase speed of the wave field,

$$c_*' = \frac{\omega'}{k_*} = \frac{N}{m_*} \tag{8}$$

and where β is the appropriate generalization of the scaled mean wind to a spectrum with a continuum of wavenumbers and phase speeds,

$$\beta = \frac{\bar{u}}{c_*'} = \frac{\bar{u} m_*}{N}. \tag{9}$$

Then (4) can be written as a function of intrinsic and observed frequencies as

$$E(\omega,\omega') = E(k,\omega')\left|\frac{\partial k}{\partial \omega}\right| = \delta(\omega'-\omega_o')\frac{((\omega-\omega')/\cos\phi)^a(\beta\omega')^{t-1}}{(\beta\omega'+(\omega-\omega')/\cos\phi)^{t+a}}. \quad (10)$$

It is now trivial, because of the delta function, to integrate over ω', with the result

$$E(\omega) = \frac{((\omega-\omega_o')/\cos\phi)^a(\beta\omega_o')^{t-1}}{(\beta\omega_o'+(\omega-\omega_o')/\cos\phi)^{t+a}}. \quad (11)$$

This solution is valid for all ϕ. Indeed, if the azimuthal distribution of wave energy were specified, it could be integrated numerically over ϕ. But since our objective in this paper is to gain an *understanding of the effects of* Doppler shifting by means of approximate, analytic solutions, we will consider only the extreme effects of Doppler shifting by choosing $\phi = 0^o$ and 180^o so that $\cos\phi = \pm 1$. Then

$$E_{\pm}(\omega) = \frac{(\pm(\omega-\omega_o'))^a(\beta\omega_o')^{t-1}}{(\beta\omega_o' \pm (\omega-\omega_o'))^{t+a}} . \quad (12)$$

The $E_+(\omega)$ spectrum holds only for $\omega \geq \omega_o'$ and vice versa.

To illustrate the sensitivity of the observed frequency spectrum to the shape of the prescribed horizontal wavenumber spectrum at small k, we select a slope of $t = 3$ at large wavenumbers, consistent with the gravity wave dispersion

relation and a saturation spectrum of gravity waves at large vertical wavenumbers (Smith et al., 1987), and consider $a = -1$, 0, and +1. These three spectra, normalized to the same energy density at large k, are shown in Figure 1. The resulting observed frequency spectra will obviously depend both on the spectral slope a and on the degree of Doppler shifting, expressed through β.

We examine this dependence by differentiating (12) to reveal the locations of the peaks in $E_{\pm}(\omega)$. These occur at

$$\omega_{max} = \begin{cases} \omega_o'(1 \pm \frac{\beta a}{t}), & a > 0 \\ \omega_o' & , a \leq 0. \end{cases} \tag{13}$$

Thus, provided that $a > 0$, the peaks are each displaced from the intrinsic frequency ω_o' by a frequency increment $\beta a \omega_o'/t$. If $a \leq 0$, the peak is unshifted, with only a spreading of energy about ω_o' occurring. Note that these results assume that all values of ω from $-\infty$ to $+\infty$ are allowed. However, observed spectra do not distinguish between positive and negative frequencies. Thus, $E(\omega<0)$ must be folded back on $E(\omega>0)$ to form $E(|\omega|)$. This will alter the observed frequency spectrum only slightly for small $\beta a/t$, but will result in significant modifications for $\beta a/t > 1$. To avoid ambiguity, the frequency spectra obtained here and in the following sections will be presented in the form $E(|\omega|)$.

The frequency spectrum, $E(|\omega|)$, obtained assuming equal up-shifted and down-shifted energies for the spectral slopes specified above and for $\beta = 1$ and 3 are shown in Figure 2 a and b. It is clear from these spectra that large energy densities at small k cause the energy to remain near ω_o' whereas small energies allow the spectral peaks to move as a result of Doppler shifting. As will be seen in the following section, however, the energy content form of the Doppler-shifted frequency spectrum, $\omega E(|\omega|)$, shows that significant energy can be Doppler shifted to higher frequencies in spite of the peak in $E(|\omega|)$ remaining near the frequency at which $E(\omega')$ is maximum.

We have provided in this section two examples of the effects of Doppler shifting on simple intrinsic frequency spectra and discussed the causes of shifts of the peak energy densities when these occurred. Our intent was to provide physical insight into the consequences of Doppler shifting of atmospheric gravity waves. Hopefully, this will assist the reader in understanding the effects of Doppler shifting on more complex spectra discussed in the following sections.

3. DOPPLER SHIFTING OF CONTINUOUS INTRINSIC FREQUENCY SPECTRA

Our intent in this section is to derive approximate expressions for the frequency spectra of horizontal and

vertical gravity wave motions arising through Doppler shifting of the intrinsic frequency spectra. As in the previous section, we will assume that the gravity wave motions are hydrostatic and two-dimensional in order to obtain analytic expressions for the Doppler-shifted spectra. We will also again assume that wave motions propagate only with or against the mean flow so that $\cos\phi = \pm 1$.

3.1 Up- and Down-Shifted Energy Densities

We begin by assuming a horizontal spectral energy density for intrinsic frequencies ω' between f and N given by

$$E^h(k,\omega') = E_o(p-1)f^{p-1}\frac{\omega'^{-p}(t-1)}{k_*(1 + k/k_*)^t}, \qquad (14)$$

where p and t are the spectral slopes. This is the same form as the two-dimensional energy spectrum used by Garrett and Munk (1975) and VanZandt (1982) except for the neglect of factors $(1 \pm (f/\omega)^2)$, consistent with the condition $\omega^2 >> f^2$ leading to (6). Here, $E_o = E_+ + E_-$ is the total energy (kinetic plus potential) and E_+ and E_- are the portions associated with gravity waves with intrinsic phase speeds $c' = \omega'/k \geq 0$ and $c' < 0$, respectively.

We assume that this spectrum is independent of the background structure of wind and temperature. Since almost nothing is known about the shape of the intrinsic frequency

spectrum, this is at present the only justifiable assumption. It is also simple and convenient. But it is unlikely to be true in general because the propagation of gravity waves is strongly affected by gradients, particularly vertical gradients, of wind and temperature. It would be a good approximation only if the processes that tend to drive the intrinsic spectrum toward an equilibrium shape were sufficiently fast.

The corresponding vertical energy density is obtained by using the continuity equation and the dispersion relation for two-dimensional gravity waves to write

$$w^2 = \frac{\omega'^2}{N^2}u^2. \qquad (15)$$

The vertical energy density is then

$$E^v(k,\omega') = E^h(k,\omega')\frac{w^2}{u^2}$$

$$= \frac{E_o}{N^2}(p-1)f^{p-1}\frac{\omega'^{2-p}(t-1)}{k_*(1+k/k_*)^t}. \qquad (16)$$

These spectra can be expressed in terms of ω and ω' by eliminating k using Eq. (2). The resulting transformed spectra are

$$E^h_{I,II}(\omega,\omega') = E^h_{I,II}(k,\omega')\left|\frac{\partial k}{\partial \omega}\right|$$

$$= \alpha_h f^p(t-1)\beta^{t-1}\frac{\omega'^{t-1-p}}{(\beta\omega' \pm (\omega-\omega')/\cos\phi)^t} \quad (17)$$

and

$$E^{v}_{I,II}(\omega,\omega') = \alpha_v f^p (t-1)\beta^{t-1} \frac{\omega'^{\,t+1-p}}{(\beta\omega' \pm (\omega-\omega')/\cos\phi)^t}, \quad (18)$$

where $\alpha_h = N^2\alpha_v = E_+(p-1)f^{-1}$. The Doppler-shifted spectra, $E^h(\omega)$ and $E^v(\omega)$, can then be evaluated by integrating over ω' from f to N. As before, there are two cases that must be considered:

$$\cos\phi = +1 \text{ and } \omega \geq \omega' \text{ (Case I)} \quad (19a)$$

and

$$\cos\phi = -1 \text{ and } \omega < \omega' \text{ (Case II).} \quad (19b)$$

In both cases $(\beta\omega' + (\omega - \omega'))$ is positive so that $(\ )^t$ is real. The different ranges of integration over ω' for each case are depicted in Figure 3. For $\omega \leq f$ or $\omega \geq N$, the limits of ω' are f and N. For $f \leq \omega \leq N$, however, the limits are f and ω for case I ($\omega \geq \omega'$) and ω and N for case II ($\omega < \omega'$). As before, since the observed spectra are in terms of $|\omega|$, the spectrum in the IIA- range must be folded back onto the positive axis to form $E(|\omega|)$. Then the contributions to $E(|\omega|)$ in each range of $|\omega|$ are given by

$$E_A(|\omega| \leq f) = E_{IIA+} + E_{IIA-} \quad (20a)$$

$$E_B(f \leq |\omega| \leq N) = E_{IB} + E_{IIB} + E_{IIA-} \quad (20b)$$

and

$$E_C(N \leq |\omega|) = E_{IC} + E_{IIA-}. \quad (20c)$$

Because both the integrands and the limits of integration in range B are different for cases I and II, we will consider each case separately from this point on. The horizontal and

vertical energy densities as functions of observed (Doppler-shifted) frequency ω for case I can be written as

$$E_I(\omega) = \int_f^{\omega_u'} E_I(\omega,\omega')d\omega', \tag{21}$$

where ω_u' (u for "upper") equals N in range C and ω in range B. Likewise, for case II

$$E_{II}(\omega) = \int_{\omega_l'}^{N} E_{II}(\omega,\omega')d\omega', \tag{22}$$

where ω_l' (l for "lower") equals ω in range B and f in range A.

In order to evaluate these integrals and determine the effects of Doppler shifting on the frequency spectra, we must specify the spectral slopes p and t. Recent atmospheric observations suggest that t = 3, due to a saturation spectrum of gravity waves (see Smith et al., 1987). Observed frequency spectra of horizontal velocities, on the other hand, exhibit considerable variability, but are most often near p = 5/3. Unfortunately, this choice does not yield integrals that can be performed analytically. For this reason, and because we do not expect the results to be sensitive to small variations in p, we choose p = 2. (It may be noted that convenience of integration was one of the reasons that Garrett and Munk(1972) chose p = 2 (Munk, private communication)!)

With the selection (p,t) = (2,3), (21) and (22) take the form

$$E(\omega) = \alpha\int x^m/(a+bx)^3dx, \tag{23}$$

with m = 0 and 2 for the horizontal and vertical spectra, respectively. The solution for the horizontal energy density (m = 0) is quite simple, with one term in each region of the form

$$\int \frac{dx}{(a+bx)^3} = -\frac{1}{2b(a+bx)^2}. \qquad (24)$$

That for the vertical energy density (m = 2) has three terms and is given by

$$\int \frac{x^2 dx}{(a+bx)^3} = \frac{1}{b^3}\left[\ln(a+bx) + \frac{2a}{a+bx} - \frac{a^2}{2(a+bx)^2} \right]. \qquad (25)$$

In particular, it is now clear that the horizontal and vertical energies will not be simply related at a given observed frequency because that relation is based on the intrinsic frequency of the motion which is, in general, unknown.

We now proceed to use (17) and (18) in (21) and (22) to obtain the expressions for up- and down-shifted horizontal and vertical energy densities. Before evaluating the integrals, however, it is convenient to express all frequencies nondimensionally by dividing all frequencies by f, ie., $\hat{x}$ = x/f.

Each region with $\omega \gtrless \omega'$ (IB and IC) contributes a term of the form (24) to the horizontal energy density and a term of the form (25) to the vertical energy density. Expressed in terms of nondimensional frequencies, these energy densities may be written

$$E_I^h(\omega) = \alpha_h \beta^2 (\hat{\omega}_u' - 1) \frac{(2\hat{\omega} + (\beta-1)(\hat{\omega}_u' + 1))}{(\hat{\omega}+\beta-1)^2 \quad (\hat{\omega}+(\beta-1)\hat{\omega}_u')^2} \tag{26}$$

and

$$E_I^v(\omega) = 2\alpha_v f^2 \frac{\beta^2}{(\beta-1)^3} \Bigg[\ln\left\{\frac{\hat{\omega}+(\beta-1)\hat{\omega}_u'}{\hat{\omega}+\beta-1}\right\}$$

$$+ \frac{3\hat{\omega}^2 + 4\hat{\omega}(\beta-1)\hat{\omega}_u'}{2(\hat{\omega}+(\beta-1)\hat{\omega}_u')^2} - \frac{3\hat{\omega}^2 + 4\hat{\omega}(\beta-1)}{2(\hat{\omega}+\beta-1)^2}\Bigg]. \tag{27}$$

Similarly, each region with $\omega < \omega'$ (IIB, IIA+, and IIA-) contributes terms of the form (24) and (25) to the horizontal and vertical energy densities, respectively. These contributions, expressed in terms of nondimensional frequencies, may be written

$$E_{II}^h(\omega) = \alpha_h \beta^2 (\hat{N} - \hat{\omega}_l') \frac{(-2\hat{\omega} + (\beta+1)(\hat{N} + \hat{\omega}_l'))}{(-\hat{\omega}+(\beta+1)\hat{\omega}_l')^2 (-\hat{\omega}+(\beta+1)\hat{N})^2} \tag{28}$$

and

$$E_{II}^v(\omega) = 2\alpha_v f^2 \frac{\beta^2}{(\beta+1)^3} \Bigg[\ln\left\{\frac{-\hat{\omega}+(\beta+1)\hat{N}}{-\hat{\omega}+(\beta+1)\hat{\omega}_l'}\right\}$$

$$+ \frac{3\hat{\omega}^2 - 4\hat{\omega}(\beta+1)\hat{N}}{2(-\hat{\omega}+(\beta+1)\hat{N})^2} - \frac{3\hat{\omega}^2 - 4\hat{\omega}(\beta+1)\hat{\omega}_l'}{2(-\hat{\omega}+(\beta+1)\hat{\omega}_l')^2}\Bigg]. \tag{29}$$

We are now in a position to determine the horizontal and vertical energy densities for any $|\omega|$ using (20), (26) - (29), and the appropriate value of $\hat{\omega}_l'$ or $\hat{\omega}_u'$ for each contribution.

3.2 The Doppler-Shifted Spectra

The Doppler-shifted horizontal energy spectrum $E^h(|\omega|)$ is obtained by substituting Eqs. (26) and (28) with the appropriate values of $\hat{\omega}_l'$ and $\hat{\omega}_u'$ into Eqs. (20a, b, and c), with $-\hat{\omega}$ replaced by $\hat{\omega}$ in the E_{IIA-} terms. The resulting expressions are

$$E_A^h(|\omega|<f) = \frac{E_-}{f}\beta^2(\hat{N}-1)\frac{(-2\hat{\omega}+(\beta+1)(\hat{N}+1))}{(-\hat{\omega}+\beta+1)^2(-\hat{\omega}+(\beta+1)\hat{N})^2}$$

$$+\frac{E_-}{f}\beta^2(\hat{N}-1)\frac{(2\hat{\omega}+(\beta+1)(\hat{N}+1))}{(\hat{\omega}+\beta+1)^2(\hat{\omega}+(\beta+1)\hat{N})^2}, \quad (30)$$

$$E_B^h(f\leq|\omega|\leq N) = \frac{E_+}{f}(\hat{\omega}-1)\frac{(2\hat{\omega}+(\beta-1)(\hat{\omega}+1))}{(\hat{\omega}+\beta-1)^2\hat{\omega}^2}$$

$$+\frac{E_-}{f}(\hat{N}-\hat{\omega})\frac{(-2\hat{\omega}+(\beta+1)(\hat{N}+\hat{\omega}))}{(-\hat{\omega}+(\beta+1)\hat{N})^2\hat{\omega}^2}$$

$$+\frac{E_-}{f}\beta^2(\hat{N}-1)\frac{(2\hat{\omega}+(\beta+1)(\hat{N}+1))}{(\hat{\omega}+\beta+1)^2(\hat{\omega}+(\beta+1)\hat{N})^2}, \quad (31)$$

and

$$E_C^h(|\omega|>N) = \frac{E_+}{f}\beta^2(\hat{N}-1)\frac{(2\hat{\omega}+(\beta-1)(\hat{N}+1))}{(\hat{\omega}+\beta-1)^2(\hat{\omega}+(\beta-1)\hat{N})^2}$$

$$+\frac{E_-}{f}\beta^2(\hat{N}-1)\frac{(2\hat{\omega}+(\beta+1)(\hat{N}+1))}{(\hat{\omega}+\beta+1)^2(\hat{\omega}+(\beta+1)\hat{N})^2}. \quad (32)$$

The Doppler-shifted vertical energy spectrum $E^v(|\omega|)$ is obtained in the same way, by substituting Eqs. (27) and (29)

into Eqs. (20a, b, and c). Because the expressions in Eqs. (27) and (29) are so lengthy, however, we express these energy densities as

$$E_A^v(|\omega|<f) = E_{II}^v(\omega;\hat{\omega}_l'=1) + E_{II}^v(-\omega;\hat{\omega}_l'=1) \ , \tag{33}$$

$$E_B^v(f\le|\omega|\le N) = E_I^v(\omega;\hat{\omega}_u'=\hat{\omega}) + E_{II}^v(\omega;\hat{\omega}_l'=\hat{\omega}) + E_{II}^v(-\omega;\hat{\omega}_l'=1), \tag{34}$$

and

$$E_C^v(|\omega|>N) = E_I^v(\omega;\hat{\omega}_u'=\hat{N}) + E_{II}^v(-\omega;\hat{\omega}_l'=1) \ . \tag{35}$$

As a check, we set $\beta = 0$ in Eqs. (30) - (35). The resulting spectra should be identical to the intrinsic frequency spectra and are given by

$$E_B^h(f\le|\omega|\le N) = \frac{(E_+ + E_-)}{f}\hat{\omega}^{-2} = \frac{E_o}{f}\hat{\omega}^{-2} \ , \tag{36}$$

$$E_C^h(N<|\omega|) = E_A^h(|\omega|<f) = 0 \ , \tag{37}$$

$$E_B^v(f\le|\omega|\le N) = (E_+ + E_-)f/N^2 \ , \tag{38}$$

and

$$E_A^v(|\omega|<f) = E_C^v(N<|\omega|) = 0 \ . \tag{39}$$

These expressions are indeed identical with the intrinsic frequency spectra.

It is also instructive to consider $E^h(|\omega|)$ when $\beta = 1$. In the middle of range B, where $f \ll \omega \ll N$, the horizontal energy density reduces to

$$E_B^h(|\omega|) \simeq \frac{(2E_+ + E_-)\hat{}}{f}\omega^{-2} . \qquad (40)$$

Thus the up-shifted portion of the gravity wave spectrum makes the predominant contribution to the enhancement of $E_B{}^h(|\omega|)$ relative to the intrinsic frequency spectrum. Likewise, the horizontal energy densities near $\omega \sim 0$ and $\omega >> N$ are

$$E_A^h(|\omega|\sim 0) \simeq \frac{E_-}{2f} \qquad (41)$$

and

$$E_C^h(|\omega|>>n) \simeq \frac{(E_+ + E_-)}{f} \frac{4\hat{N}}{\hat{\omega}^3}. \qquad (42)$$

Only the down-shifted wave energy contributes for $|\omega| < f$ while the up- and down-shifted energies contribute nearly equally for $|\omega| >> N$. Also, the energy density at large $|\omega|$ decays rapidly with increasing $|\omega|$, as expected. These characteristics of the Doppler-shifted frequency spectra, as well as their dependence on β and anisotropy, are addressed in detail in the following section.

4. DISCUSSION OF DOPPLER-SHIFTED SPECTRA

We present in this section a variety of results obtained from the horizontal and vertical Doppler-shifted spectra derived in the preceding section. Our objectives here are to illustrate the various effects of Doppler shifting on the

horizontal and vertical frequency spectra as a function of the scaled mean wind β and to point out some of the errors in interpretation that may occur if the effects of Doppler shifting are not properly taken into account. For the most part, we consider only components of the gravity wave spectrum that propagate with or opposed to the mean flow, recognizing that the components propagating perpendicular to $\bar{u}$ are unaffected by Doppler shifting. Thus, our two-dimensional spectra can be viewed as upper limits to the effects of Doppler shifting, with the energy density for orthogonal wave motions corresponding to the case $\beta = 0$.

In order to compute the Doppler-shifted energy spectra we must specify E_+/E_-, N/f, and β. In most cases we assume that the two-dimensional gravity wave spectrum is symmetric so that $E_+/E_- = 1$. For N/f we use a nominal value of 100, which is appropriate in the troposphere at middle and high latitudes. We also note that $\beta = \bar{u}/(N/m_*)$ ranges from 0 to a maximum value that is uncertain principally due to the uncertainty in the value of m_*. With the smallest values that have been quoted, 0.5 - 1.0 $\times 10^{-3}$ cyc/m in the troposphere and lower stratosphere (see Smith et al., 1987), β can be as large as $\sim$ 10. Therefore, the resulting two-dimensional, Doppler-shifted horizontal and vertical frequency spectra are shown in Figure 4 for $\beta = 0$, 0.8, 2, 5, and 10.

Several features of the Doppler-shifted frequency spectra are immediately apparent. First, the peak in the frequency spectrum of horizontal energy (Figure 4a) remains near $\hat{\omega} = 1$ ($\omega = f$) as β increases, as anticipated in Section 2 for a horizontal wavenumber distribution of the form used here. Again, this is a result of the finite energy density at very large horizontal scales for which Doppler shifting has a negligible effect on the observed frequencies. Also evident in Figure 4 are significant modifications in spectral shape, including changes in spectral power and slope at all frequencies. There is a tendency for the slope of the horizontal frequency spectrum to increase (toward positive values) as β increases, though only weakly near N. Accompanying this change in slope is an increase in horizontal energy density at higher frequencies and a corresponding reduction near f due to the preferential Doppler shifting of energy to higher observed frequencies. In contrast, the frequency distribution of vertical motions is seen to undergo decreases in slope (toward negative values) and in power at higher frequencies. This occurs because the majority of the vertical energy resides at high intrinsic frequencies and is easily Doppler shifted to observed frequencies with $|\omega| > N$.

To illustrate the sensitivity of the observed energy density to small β, we examine the form of $E_B^h(|\omega|)$ for β and $1 << \hat{\omega} << \hat{N}$. Also assuming $E_+ = E_-$, (30) yields

$$E_B^h(|\omega|) \simeq \frac{E_o}{f\omega^2}(1+\beta^2/(1+\beta)). \tag{43}$$

For small β, $E_B{}^h(|\omega|)$ increases as β^2 because changes due to Doppler shifting are largely off-setting for the up- and down-shifted components. For larger β, the increase becomes linear because both up- and down-shifted components now transfer energy primarily to higher frequencies. The increases for this isotropic, two-dimensional gravity wave spectrum are 0.5, 1.33, and 2.25 for β = 1, 2, and 3. The fractional increases would be only half as large, however, had we assumed equal gravity wave energy propagating zonally and meridionally.

The fractional changes in the horizontal and vertical energy densities are shown for the different values of β in Figure 5. These curves imply a systematic increase in the ratio $E^h(|\omega|)/E^v(|\omega|)$ for $|\omega| \sim N$ as β increases. This reduction in $E^v(|\omega|)$ and increase in $E^h(|\omega|)$ at higher frequencies constitutes a departure from the ratio of horizontal to vertical energies expected for gravity waves at high intrinsic frequencies. Such a departure could lead to incorrect inferences concerning the nature of the motion spectrum if the effects of Doppler shifting are not taken into account. It should be noted that enhancements in the ratio of horizontal to vertical energy densities at higher frequencies and negative slopes of the frequency spectrum of vertical

energy have been observed in situations of nonzero mean winds (Gage and Nastrom, 1985; Rottger,1981).

A more insightful presentation of spectral results, in many respects, is the energy content spectrum, $\omega E(\omega)$ (see VanZandt, 1985). The Doppler-shifted horizontal and vertical frequency spectra for $\beta = 0$, 0.8, 2, 5, and 10 are presented in this form in Figure 6. These spectra give a more accurate indication of the distribution of energy density by accounting for the increase in frequency intervals with ω.

Considering first the horizontal energy content spectra, $\omega E^h(|\omega|)$ (Figure 6a), we see that, whereas the peak in $E^h(|\omega|)$ remains near f, the frequency at which the maximum energy occurs shifts from f at $\beta = 0$ to $\sim$ 10f at $\beta \sim 10$. This illustrates much more clearly the shift of energy toward higher frequencies due to Doppler shifting. It is also clear that a minor, though not insignificant, fraction of the horizontal energy is Doppler-shifted to $|\omega| > N$ for large β and that relatively less energy appears at $|\omega| < f$ than indicated by the horizontal energy spectra in Figure 5.

The vertical energy content spectra, $\omega E^v(|\omega|)$, shown in Figure 6b are likewise very instructive. First, this graph shows that very little energy is Doppler shifted to frequencies less than f, as might be erroneously inferred from Figure 4b. Instead, it is clear that a major fraction of the

vertical gravity wave energy can be Doppler shifted to $|\omega| > N$ at larger values of β. While the peak horizontal energy is Doppler shifted to $|\omega| \sim 10f$ at $\beta = 10$, the peak vertical energy density is shifted to $|\omega| \sim 2N$. Thus measurements of vertical gravity wave energy with a Nyquist frequency near N will alias or exclude a significant fraction of the vertical energy at large β. As discussed earlier, the more severe effects of Doppler shifting on the frequency spectrum of vertical wave energy are a consequence of the occurrence of a majority of the vertical energy at high intrinsic frequencies.

We now examine separately the up-shifted and down-shifted contributions to the energy content spectra shown in Figure 6. These are illustrated for $\beta = 2$ and 5 and compared with the intrinsic ($\beta = 0$) spectra in Figures 7 and 8. One motivation for considering each component of the gravity wave spectrum separately is that the spectrum is often highly anisotropic (Vincent and Stubbs, 1977; Manson et al., 1979; Fritts and Vincent, 1987; Vincent and Fritts, 1987) and may, on occasion, be best characterized by only the up-, down-, or un-shifted component.

For both horizontal and vertical energy spectra, the major contribution to departures from the intrinsic frequency spectrum is the up-shifted portion of the gravity wave spectrum because the fractional change in $|\omega|$ is larger for

motions with $\omega > \omega'$. For example, for gravity waves with the characteristic horizontal wavenumber $k_* = \omega'/c_*'$, we see from (2), with $\beta = 2$, that

$$\omega_{up} = \omega' + k_*\bar{u} = 3\omega' \qquad (44)$$

while

$$\omega_{down} = \omega' - k_*\bar{u} = -\omega'. \qquad (45)$$

Here the up-shifted component changes by a factor $\beta+1$ while the down-shifted component changes by $\beta-1$. The frequency difference is enhanced for $c > c_*'$ and reduced for $c < c_*'$, with the difference between up- and down-shifted components remaining the same as β increases. However, the relative frequency change for up-shifted and down-shifted components is reduced as β increases, with both components ultimately contributing to a shift toward higher Doppler-shifted frequencies.

Finally, we present in Figure 9 the area-preserving energy content spectra for $0 \leq \beta \leq 100$. (Values greater than ~ 10 are unlikely to be realized, but are included to address the limiting behavior.) These spectra show quantitatively the fraction of energy for a symmetric two-dimensional gravity wave spectrum that is Doppler shifted to frequencies outside the allowed range of intrinsic frequencies ($|\omega| < f$ and $|\omega| > N$). For $\beta = 2$ and 5, these fractions are both ~ 0.20 for the

horizontal energy and ~ 0.30 and 0.50 for the vertical energy. Once again, because most of the vertical gravity wave energy lies near $\omega' \sim N$, estimates of the vertical gravity wave energy are more likely to be biased by Doppler-shifting effects than are estimates of the horizontal energy. It is also evident from Figure 9 that as β becomes large the spectra for $\omega > N$ evolve toward a constant shape, which can be shown to be $E_0(\omega/\beta)/(1 + \omega/\beta)^2$. This can be understood by recognizing that for $\beta >> 1$, $\bar{u} >> c_*'$, implying that the wave motions are effectively imbedded in a high-speed flow with the frequency spectra given approximately by a Taylor transformation of the horizontal wavenumber spectrum. This explanation is consistent with the shift of the peak in the horizontal energy density to $|\omega| \sim \beta f$ for $\beta >> 1$. A similar shift of the peak vertical energy density to $|\omega| \sim \beta N/5$ is also observed.

5. SUMMARY AND CONCLUSIONS

We have presented a simple discussion of the consequences of a nonzero mean flow for the observed frequency spectra of gravity waves with prescribed intrinsic frequency and wavenumber spectra. In order to illustrate the effects of Doppler shifting as simply as possible, we wanted to present analytic solutions. For this reason, we elected to consider

idealized gravity wave motions and spectra. We also chose to consider only gravity waves propagating in the direction of, or opposed to, the mean flow since these two cases establish the limits of possible Doppler-shifting effects. Finally, we assumed that the shape of the intrinsic spectrum is independent of the background wind and temperature structure. In spite of these approximations, we believe that the results of this study provide a number of insights into the role of a nonzero mean wind in determining the observed frequency spectra of horizontal and vertical gravity wave energy in the atmosphere.

To examine the dependence of the observed frequency spectra on the distribution of gravity wave energy with horizontal wavenumber (or phase speed), we considered in Section 2 a distribution with intrinsic frequency of the form $E(\omega') = \delta(\omega'-\omega_o')$. For wavenumber spectra with energy localized near a dominant horizontal wavenumber, Doppler shifting was seen to result in frequency spectra with two peaks located near $\omega \sim (1\pm\beta)\omega_o'$ resulting, respectively, from the up- and down-shifted components of the gravity wave spectrum. For gravity wave spectra that have sufficient energy density at small k, however, both up- and down-shifted energy densities are spread about $\omega = \omega_o'$ because the finite energy at very small k remains virtually unaffected by Doppler

shifting. It is important to stress, however, that the energy content forms of the Doppler-shifted frequency spectra, $\omega E(|\omega|)$, do exhibit an increase in the frequency at which the maximum energy occurs as β increases. This is because the energy spectra, $E(|\omega|)$, do not account for the increasing density of frequencies at larger ω.

In Section 3 we considered the effects of Doppler shifting on an energy spectrum similar to the Garrett and Munk (1975) spectrum, which has been shown to be a reasonable approximation to the observed atmospheric spectrum (VanZandt, 1982). The results were seen to be in qualitative agreement with the results just reviewed. The peaks of the Doppler-shifted frequency spectra of horizontal and vertical energy both remained near the peaks of the intrinsic frequency energy densities as β increased due to the assumed constant value of $E(k)$ at small k. But like the results with more simplified intrinsic frequency spectra, the peak energy, $\omega E(|\omega|)$, was seen to shift toward large ω for large β, with the peak values occurring near $\omega \sim \beta f$ and $\beta N/5$ for the horizontal and vertical energy spectra, respectively. At sufficiently large β, the spectra were seen to be given approximately by a Taylor transformation of the horizontal wavenumber spectrum by the large mean wind.

For values of β representative of the lower and middle atmosphere ($\beta \lesssim 5$), Doppler shifting was found to cause significant asymmetries in the up- and down-shifted components of the resulting frequency spectra. Changes induced in the up- and down-shifted components were seen to be largely off-setting for $\beta \lesssim 1$, while both components contributed to changes of the same form for $\beta \gtrsim 2$.

Because the shapes of the horizontal and vertical intrinsic frequency spectra are quite different, the effects of Doppler shifting on the two spectra are quite different. For $|\omega| \sim N$, the horizontal energy density was seen to increase due to a transfer of energy from $\omega' \sim f$ to higher $|\omega|$. On the other hand, the vertical energy density was found to decrease in the same range of $|\omega|$ due to the transfer of energy away from $\omega' \sim N$ largely to $|\omega| > N$. These effects contributed to a change in the shape of both horizontal and vertical energy spectra and to a large increase in $E^h(|\omega|)/E^v(|\omega|)$ near $|\omega| \sim N$, consistent with frequency spectra observed in the atmosphere.

Although Doppler shifting must have effects such as those described in this paper, the shapes of $E^h(|\omega|)$ and $E^v(|\omega|)$ spectra that have been observed when $\bar{u}$ (and β) are appreciable are usually not similar to the model spectra. There are several reasons for this. First, the observed spectra are

contaminated by processes other than gravity waves, particularly at low frequencies. The horizontal spectra are contaminated by planetary wave activity, while the vertical spectra may be contaminated by the vertical motions in slowly varying mountain lee waves or potentially by the projection of essentially horizontal motions into the vertical by sloping isentropic surfaces. Second, our formulation of the effects of Doppler shifting is highly idealized. Model spectra suitable for comparison with observed spectra would include the full gravity wave dispersion relation, allow for azimuthal wave propagation, and permit more realistic intrinsic frequency spectra. Indeed, Scheffler and Liu (1986) have developed the formalism for such calculations. Such a study, however, is obviously beyond the scope and intention of this paper.

Acknowledgments

Support for one of the authors (DCF) was provided by the Air Force Office of Scientific Research under grant AFOSR-82-0125 and the Division of Atmospheric Sciences of the National Science Foundation under grant ATM-8404017. The authors would like to thank Drs. S. Fukao and T. Sato and two anonamous reviewers for helpful comments and suggestions.

6. REFERENCES

Dewan, E.M., R.E. Good, Saturation and the "universal" spectrum for vertical profiles of horizontal scalar winds in the atmosphere, J. Geophys. Res., 91, 2742-2748, 1986.

Fritts, D.C., Gravity wave saturation in the middle atmosphere: A review of theory and observations, Rev. Geophys. Space Phys., 22, 275-308, 1984.

Fritts, D.C., and P.K. Rastogi, Convective and dynamical instabilities due to gravity wave motions in the lower and middle atmosphere: Theory and observations, Radio Sci., 20, 1247-1277, 1985.

Fritts, D.C., and R.A. Vincent, Mesospheric momentum flux studies at Adelaide, Australia: Observations and a gravity wave/tidal interaction model, J. Atmos. Sci., in press, 1987.

Fukao, S., Y. Maekawa, T. Sato, and S. Kato, Fine structure in mesospheric wind fluctuations observed by the Arecibo UHF Doppler radar, J. Geophys. Res., 90, 7547-7556, 1985.

Gage, K.S., and G.D. Nastrom, On the spectrum of atmospheric velocity fluctuations seen by MST/ST radar and their interpretation, Radio Sci., 20, 1339-1347, 1985.

Garrett, C.J.R., and W.H. Munk, Space-time scales of internal waves, Geophys. Astrophys. Fluid Dyn., 3, 225-235, 1972.

Garrett, C.J.R., and W.H. Munk, Space-time scales of internal waves: A progress report, J. Geophys. Res., 80, 291-297, 1975.

Manson, A.H., C.E. Meek, and R.J. Stening, The role of atmospheric waves (1.5 hr - 10 days) in the dynamics of the mesosphere and lower thermosphere at Saskatoon (52^{o}N, 107^{o}W) during four seasons of 1976, J. Atmos. Terres. Phys., 41, 325-335, 1979.

Meek, C.E., I.M. Reid and A.H. Manson, Observations of mesospheric wind velocities. I. Gravity wave horizontal scales and phase velocities determined from spaced wind observations, Radio Sci., 20, 1363-1382, 1985a.

Meek, C.E., I.M. Reid and A.H. Manson, Observations of mesospheric wind velocities. II. Cross sections of power spectral density for 48-8h, 8-1h, 1h-10 min over 60-110 km for 1981, Radio Sci., 20, 1383-1402, 1985b.

Palmer, T.N., G.J. Shutts, and R. Swinbank, Alleviation of a systematic westerly bias in general circulation and numerical weather prediction models through an orographic gravity wave drag parameterization, Quart. J. Roy. Met. Soc., 112, 1001-1039, 1986.

Rottger, J., Wind variability in the stratosphere deduced from spaced antenna VHF radar measurements, Proc. 20th Conf. on Radar Meteorology, Boston, 22-29, 1981.

Scheffler, A.O., and C.H. Liu, On observation of gravity wave spectra in the atmosphere by using MST radars, Radio Sci., 20, 1309-1322, 1985.

Scheffler, A.O., and C.H. Liu, The effects of Doppler shift on the gravity wave spectra observed by MST radar, J. Atmos. Terres. Phys., 48, 1225-1231, 1986.

Smith, S.A., and D.C. Fritts, Estimations of gravity wave motions, momentum fluxes and induced mean flow accelerations in the winter mesosphere over Poker Flat, Alaska, Proceedings of the 21st Conference on Radar Meteorology, Edmonton, 104-110, 1983.

Smith, S.A., D.C. Fritts, and T.E. VanZandt, Comparison of mesospheric wind spectra with a gravity wave model, Radio Sci., 20, 1331-1338, 1985.

Smith, S.A., D.C. Fritts, and T.E. VanZandt, Evidence of a saturation spectrum of atmospheric gravity waves, J. Atmos. Sci., in press, 1987.

VanZandt, T.E., A universal spectrum of buoyancy waves in the atmosphere, Geophys. Res. Lett., 9, 575-578, 1982.

VanZandt, T.E., A model for gravity wave spectra observed by Doppler sounding systems, Radio Sci, 20, 1323-1330, 1985.

Vincent, R.A., and D.C. Fritts, A morphology of gravity waves in the mesosphere and lower thermosphere over Adelaide, Australia, J. Atmos. Sci., in press, 1987.

Vincent, R.A., and I.M. Reid, HF Doppler measurements of mesospheric momentum fluxes, J. Atmos. Sci., 40, 1321-1333, 1983.

Vincent, R.A., and T.J. Stubbs, A study of motions in the winter mesosphere using the pertial reflection drift technique, Planet. Space Sci., 25, 441- , 1977.

Figure Captions

1. Distributions of energy with horizontal wavenumber, $E(k)$, for low-wavenumber slopes of $a = -1$, 0, and 1.

2. Distributions of energy with Doppler-shifted frequency, $E(|\omega|)$, for low-wavenumber slopes of $a = -1$, 0, and 1 and (a) $\beta = 1$ and (b) 3. Note the separation of up- and down-shifted energy peaks for $a > 0$.

3. Regions of integration in the (ω,ω') plane for the up-shifted and down-shifted components of the horizontal and vertical frequency spectra.

4. Horizontal (a) and vertical (b) energy densities, $E^h(|\omega|)$ and $E^v(|\omega|)$, for $E_+ = E_-$ and $\beta = 0$, 0.8, 2, 5, and 10.

5. Energy density ratio, $E^h(|\omega|)/E^v(|\omega|)$, for the parameters in Figure 4. Note the large enhancement in this ratio at higher ω due to Doppler shifting.

6. Energy content spectra, $\omega E^h(|\omega|)$ and $\omega E^v(|\omega|)$, of the horizontal (a) and vertical (b) energy densities for the parameters in Figure 4. Note the shift of energy to higher frequencies.

7. Horizontal (a) and vertical (b) energy content spectra for up-shifted, down-shifted, and symmetric (2D) gravity wave spectra for $\beta = 2$.

8. As in Figure 7, but for $\beta = 5$.

9. Area-preserving energy content spectra for horizontal (a) and vertical (b) energies for the parameters in Figure 4. At large β, the distributions tend toward an invariant quasi-Guassian shape that can be interpreted as a Taylor transformation of the horizontal wavenumber spectrum.

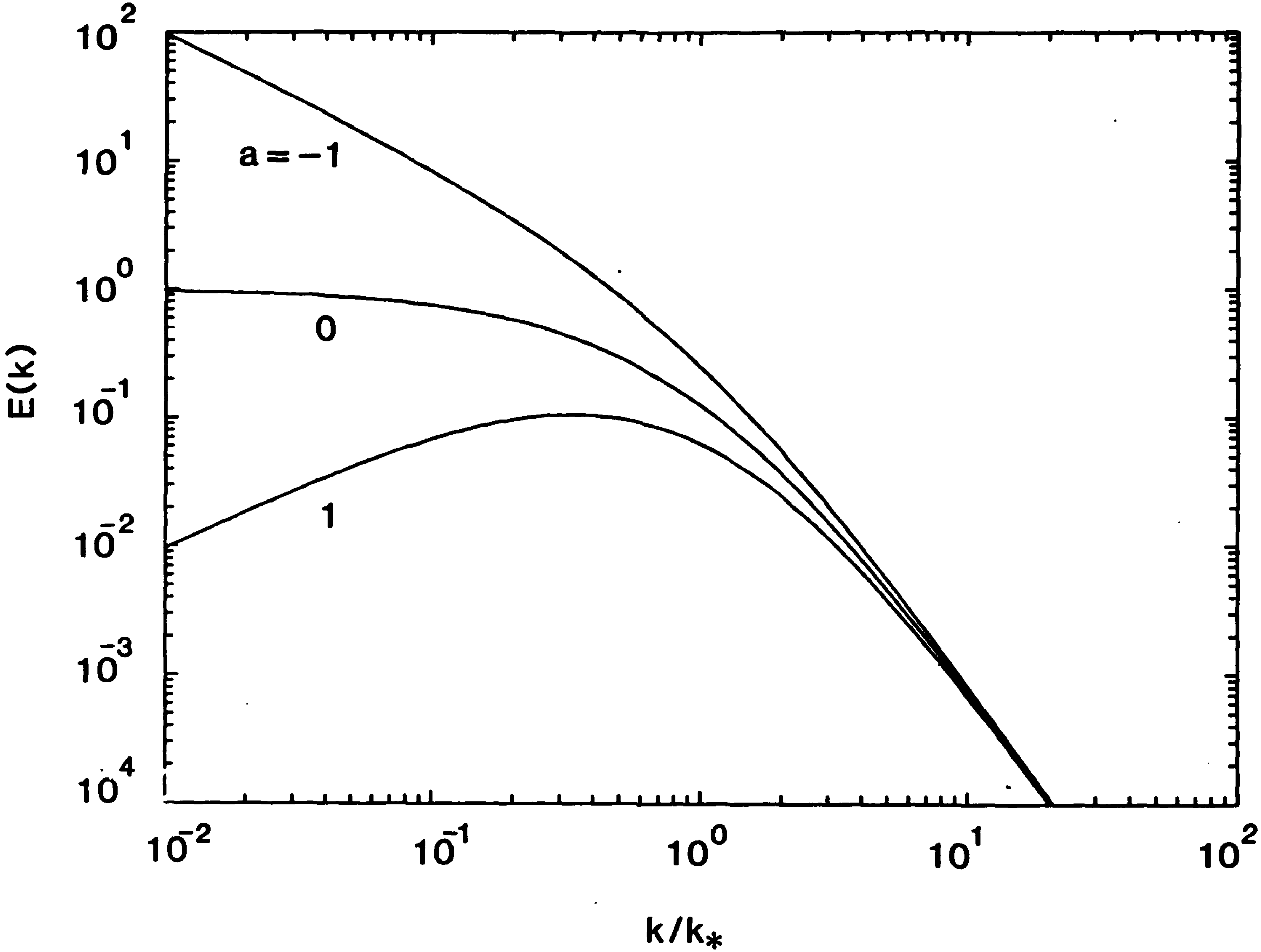

Fig. 1

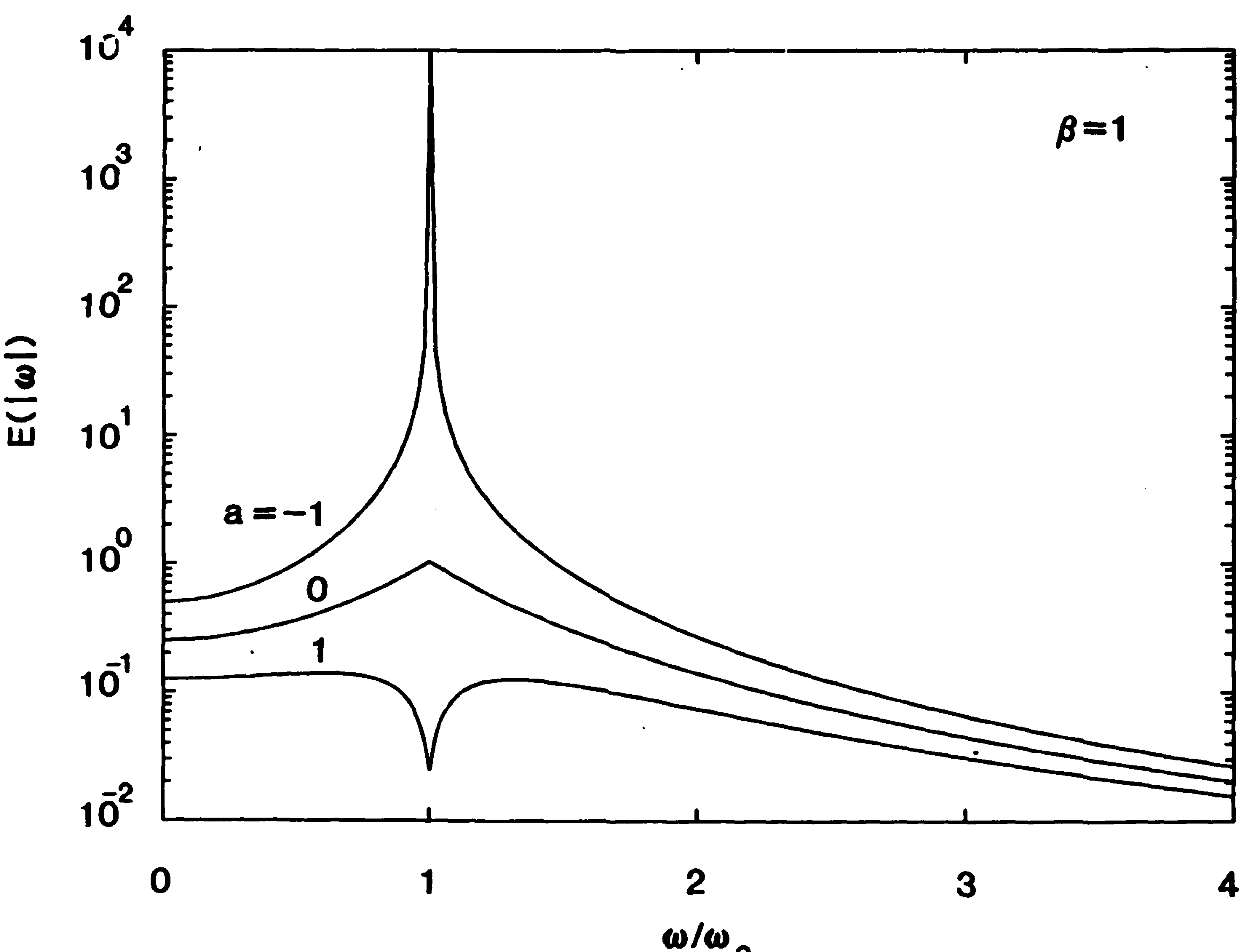

10^4
10^3
10^2
10^1
10^0
10^{-1}
10^{-2}
$E(|\omega|)$
$\beta=1$
$a=-1$
0
1
0
1
2
3
4
ω/ω_0

Fig. 2a

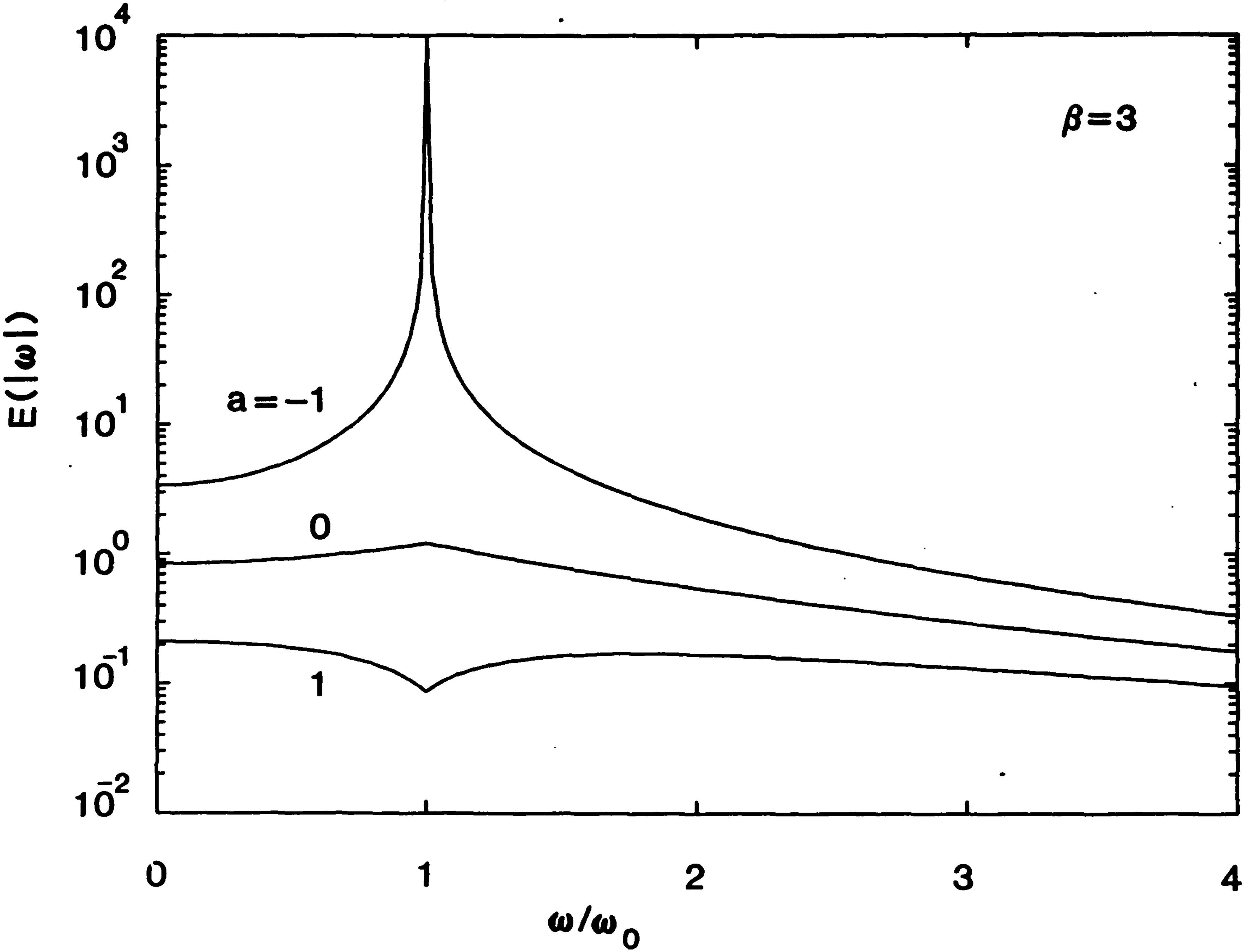

Fig. 2b

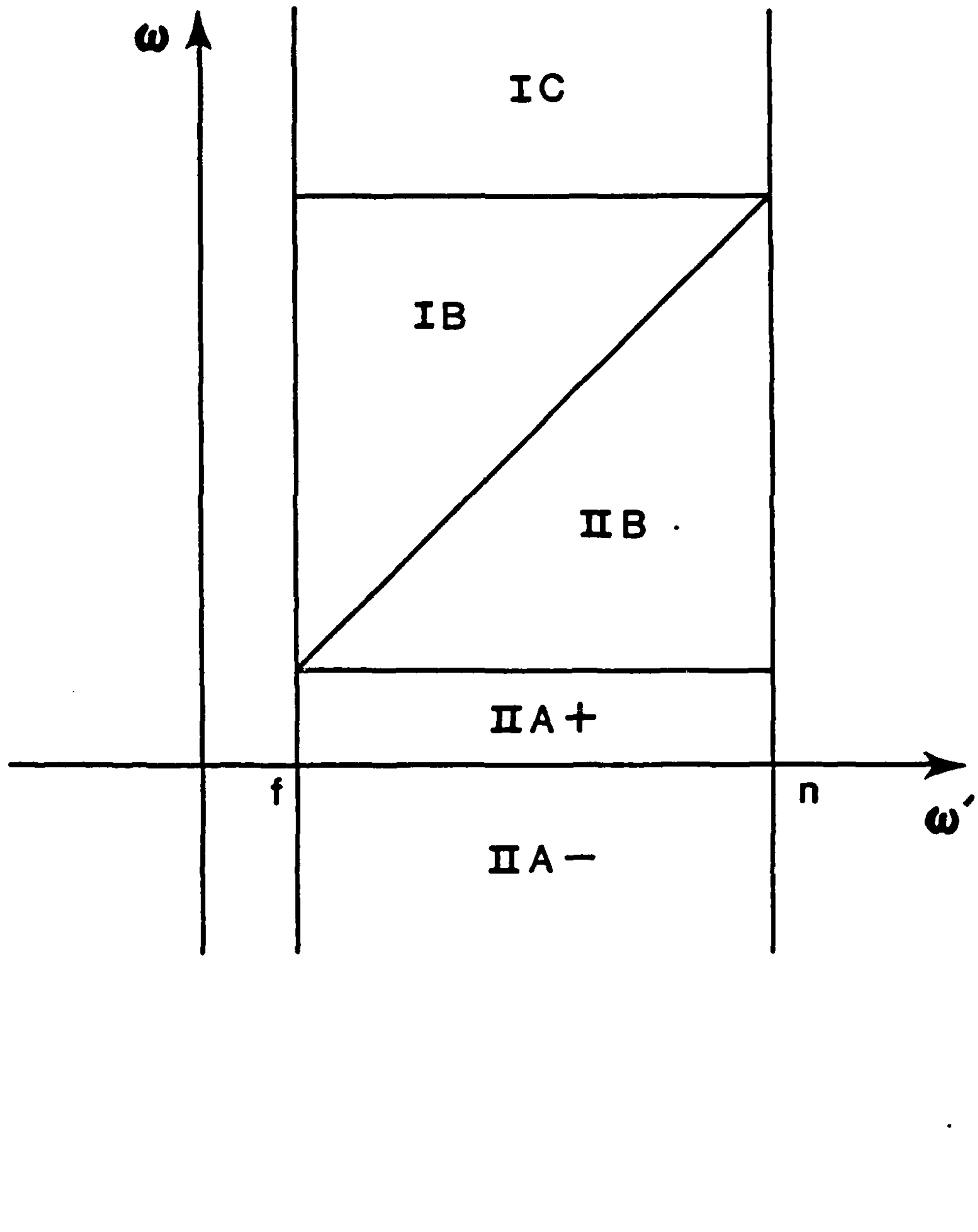

Fig. 3

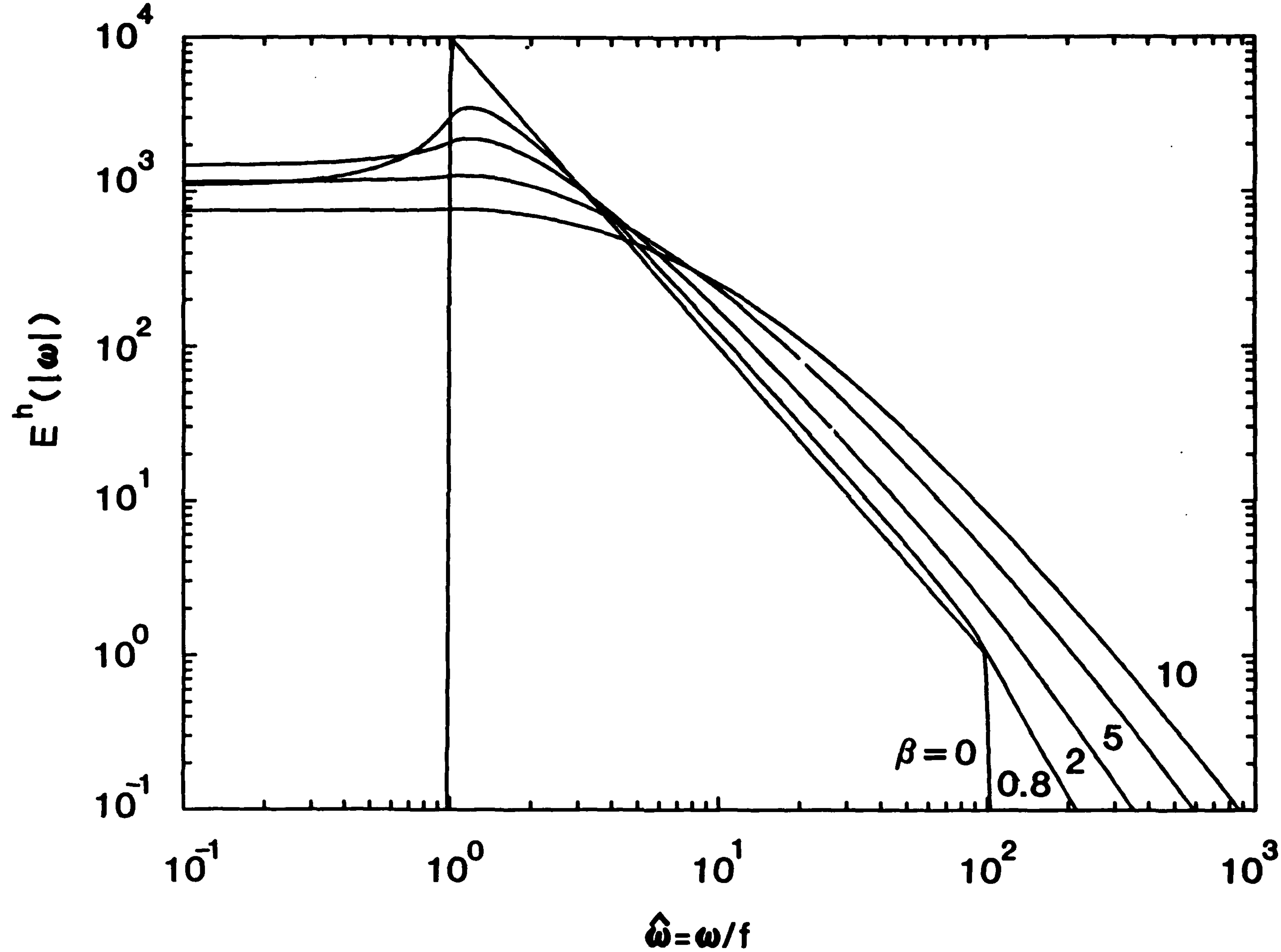

Fig. 4a

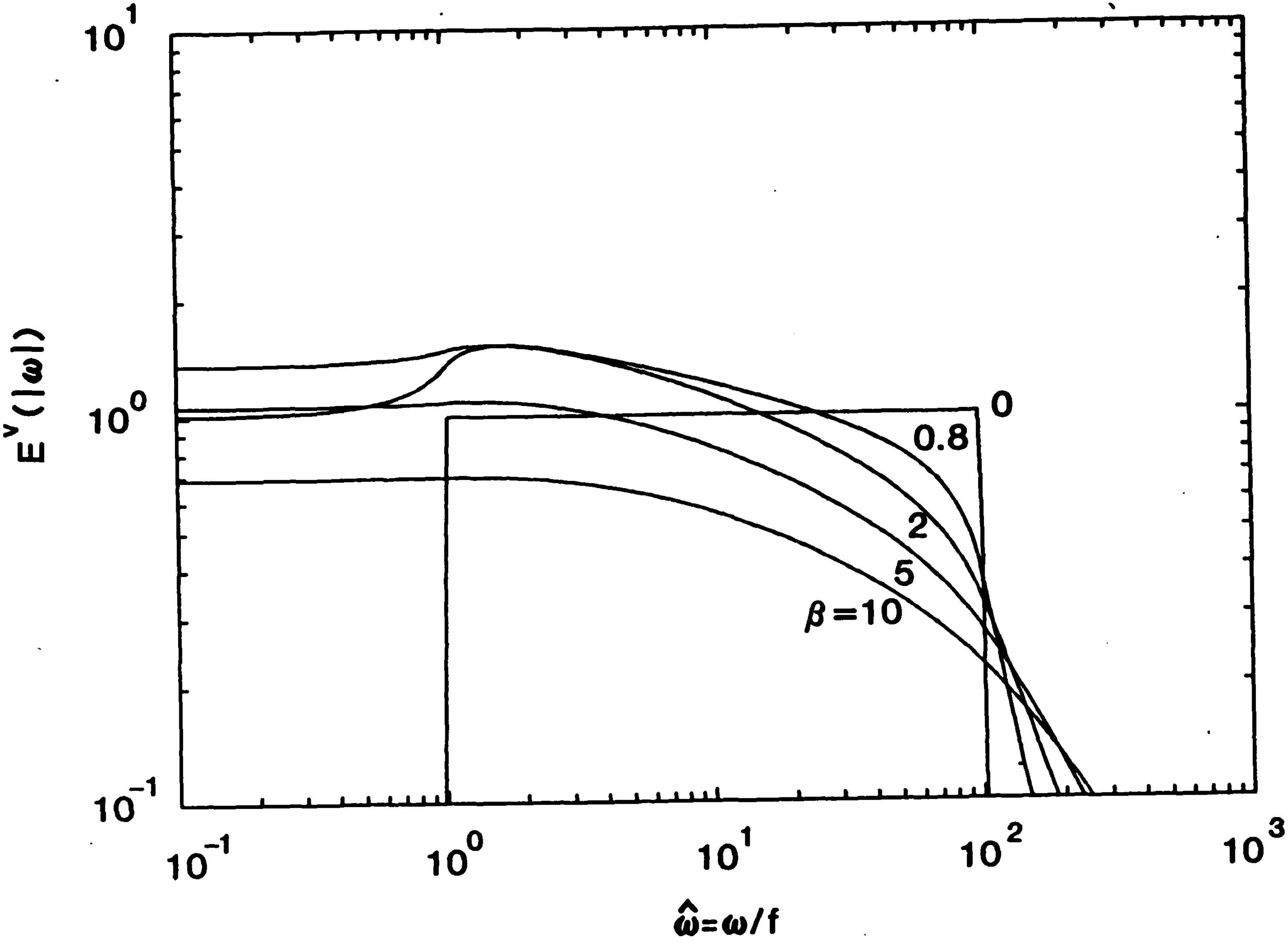

Fig 4b

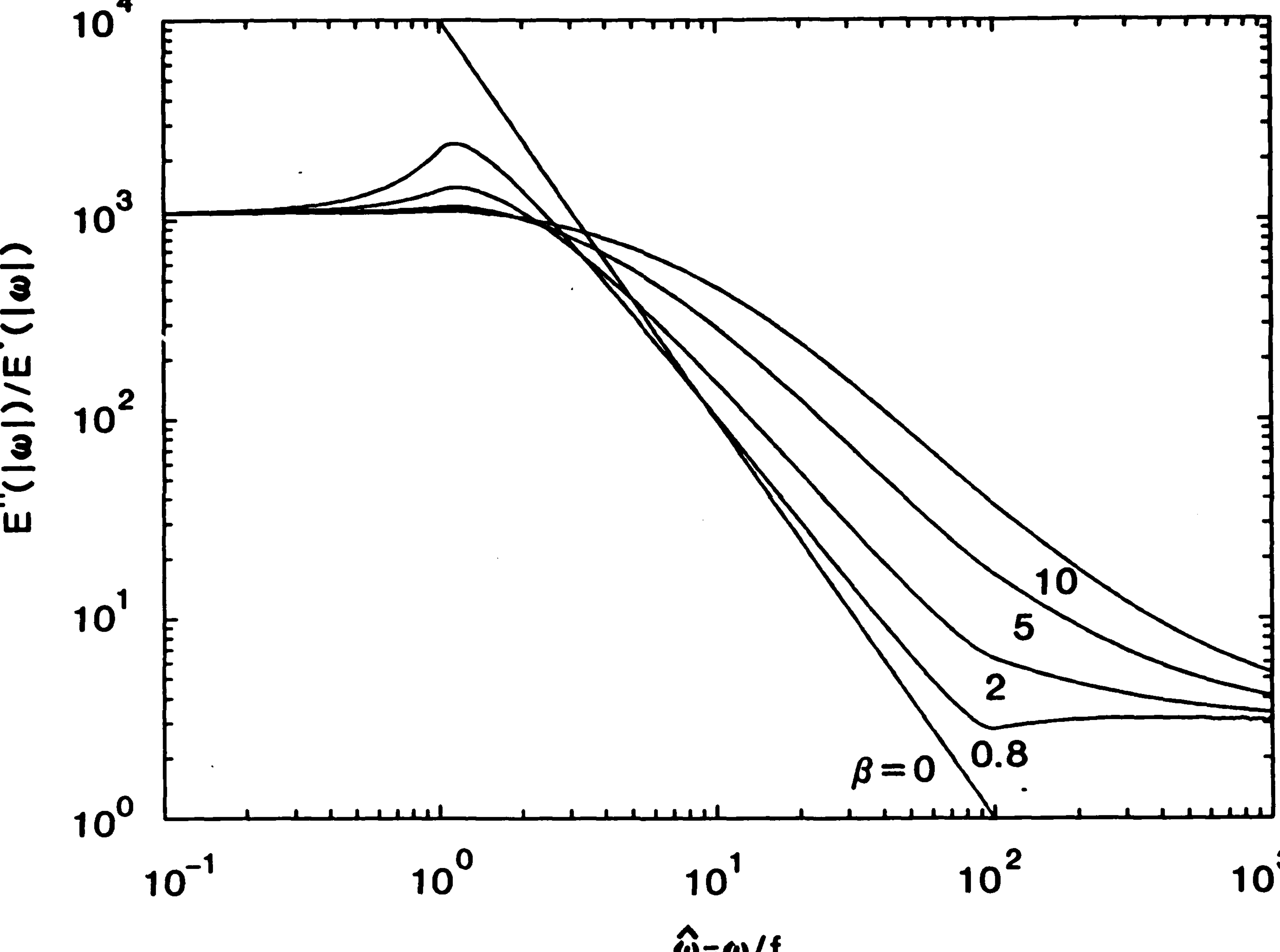

10^4
10^3
10^2
10^1
10^0
$E^h(|\omega|)/E^v(|\omega|)$
10
5
2
0.8
$\beta=0$
10^{-1}
10^0
10^1
10^2
10^3
$\hat{\omega}=\omega/f$

Fig. 5

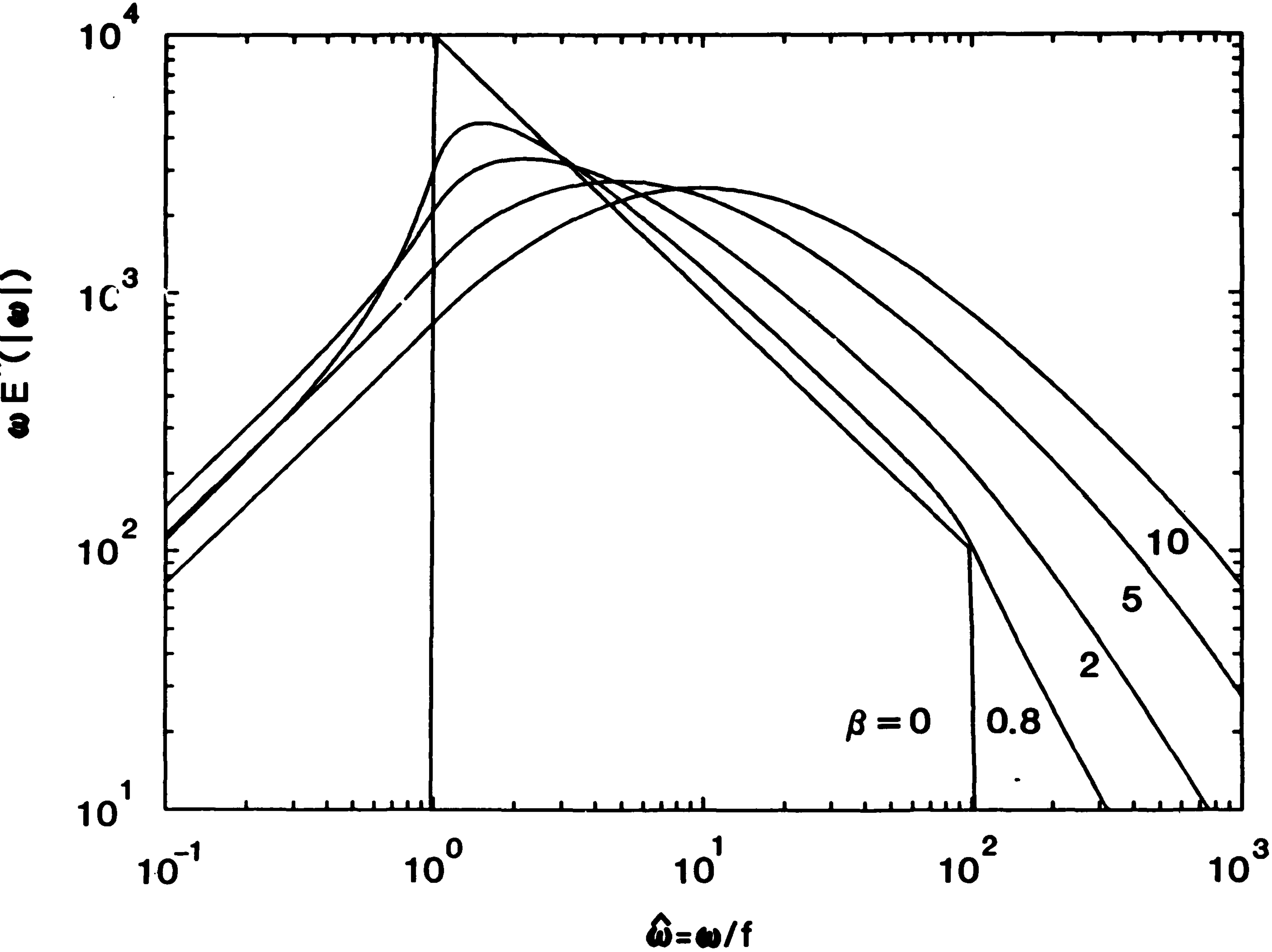

$\omega E^h(|\omega|)$
10^4
10^3
10^2
10^1
10^{-1}
10^0
10^1
10^2
10^3
$\hat{\omega}=\omega/f$
$\beta=0$
0.8
2
5
10

Fig. 6a

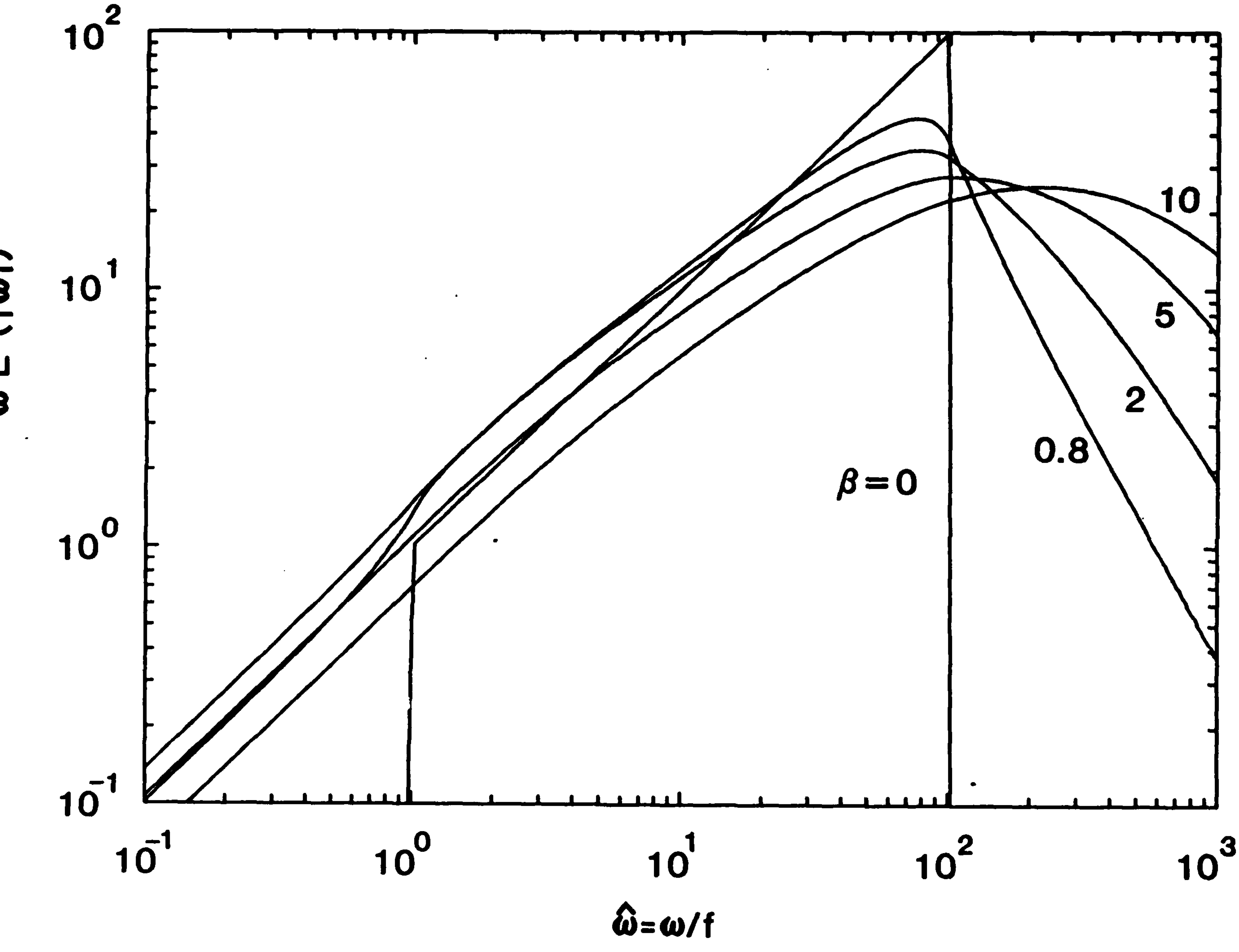
10^2
10^1
10^0
10^{-1}
$\omega E^v(|\omega|)$
10^{-1}
10^0
10^1
10^2
10^3
$\hat{\omega}=\omega/f$
$\beta=0$
0.8
2
5
10

Fig. 6 b

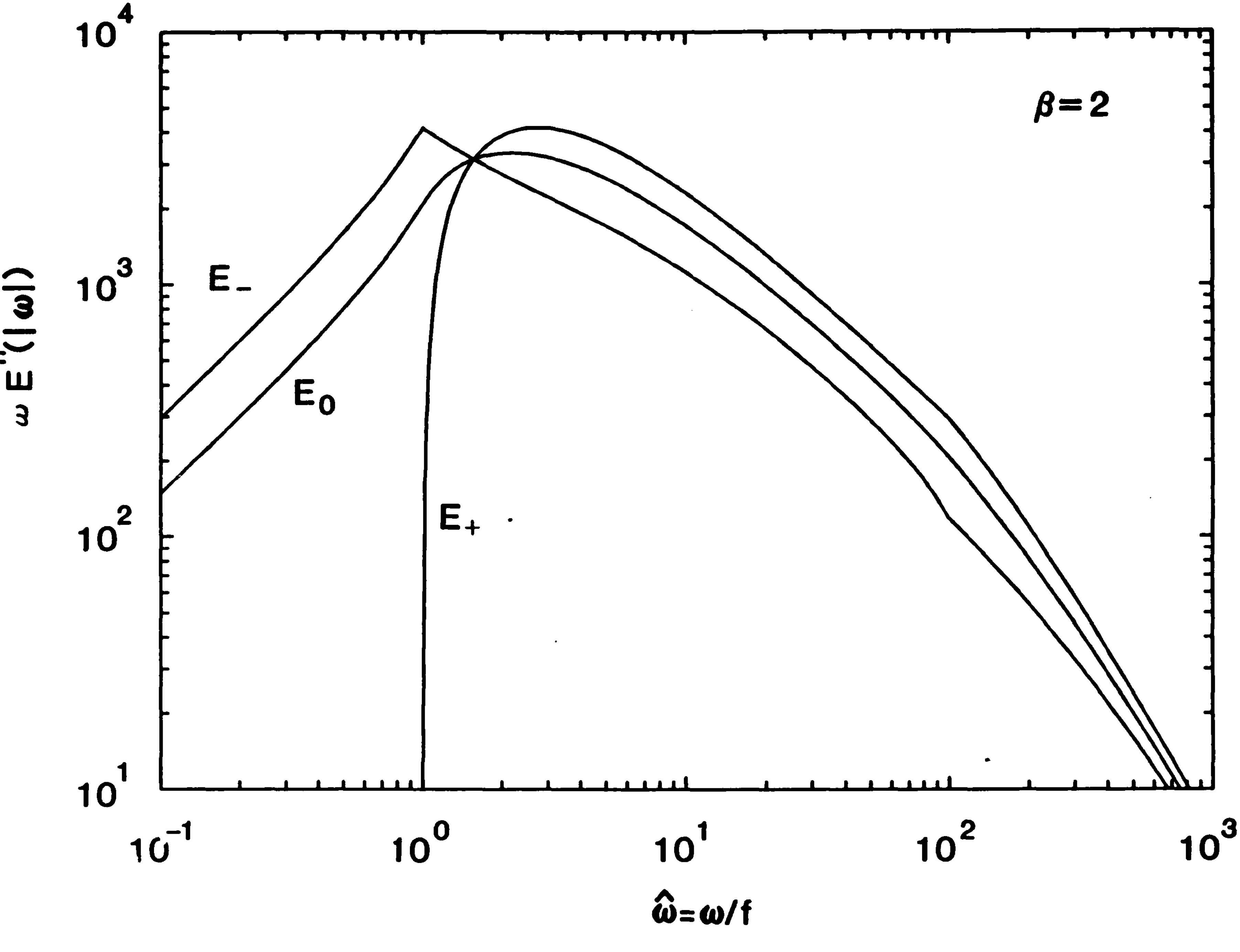

$\beta=2$
E_-
E_0
E_+
$\omega E^h(|\omega|)$
$\hat{\omega}=\omega/f$
10^4
10^3
10^2
10^1
10^{-1}
10^0
10^1
10^2
10^3

Fig. 7a

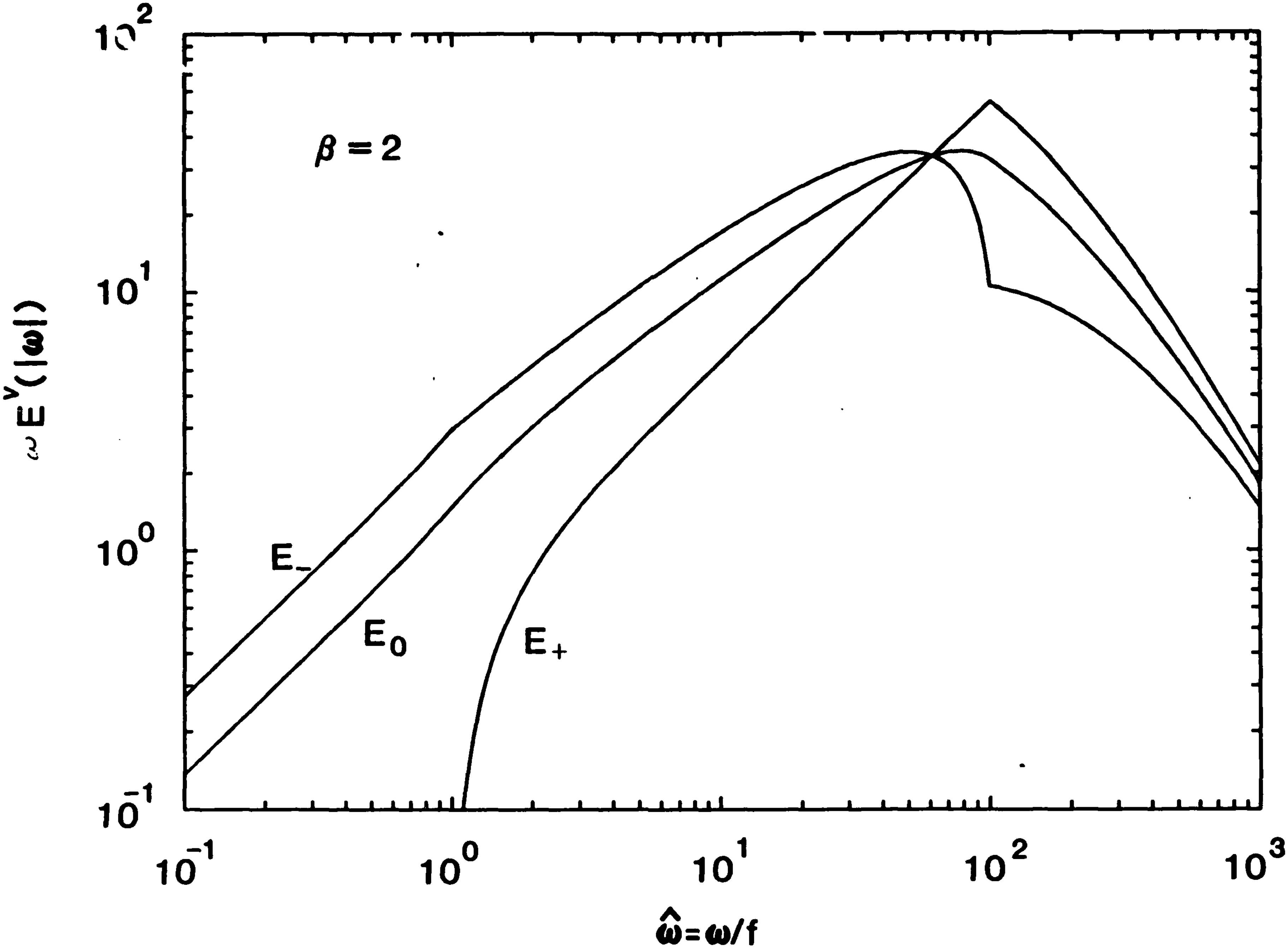

Fig. 7b

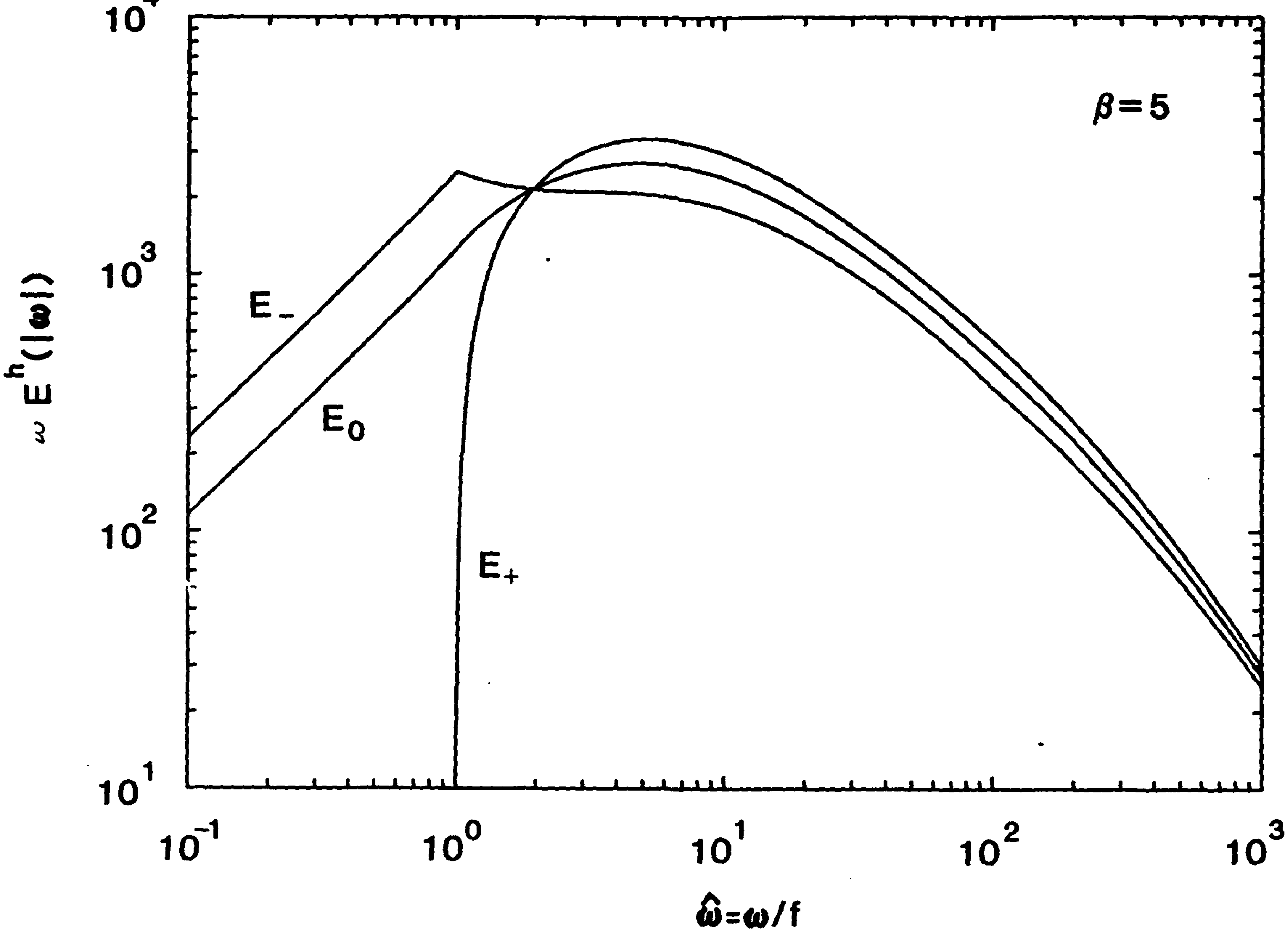

Fig. 8a

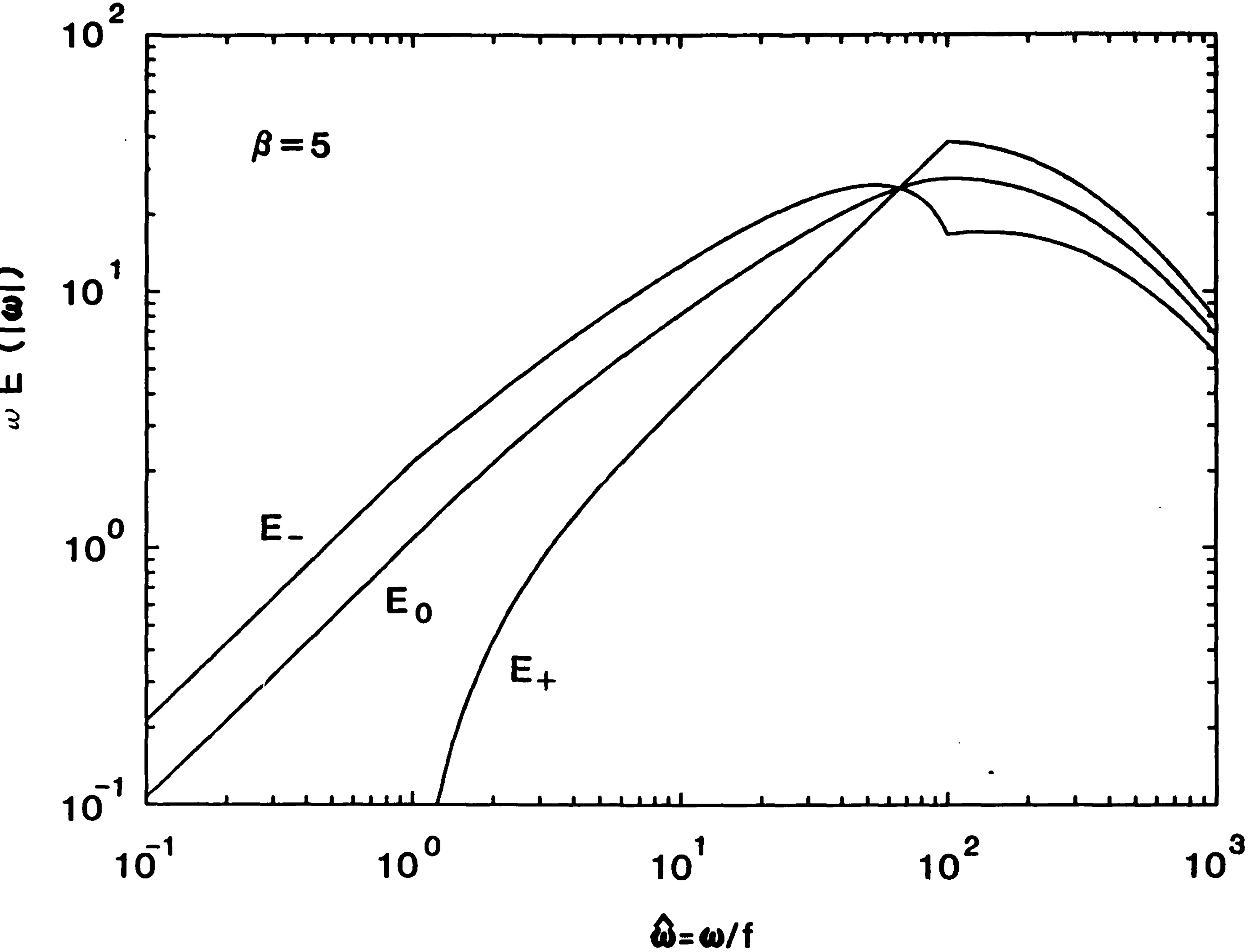
$\beta = 5$
E_-
E_0
E_+
$\omega E^v(|\omega|)$
$\hat{\omega} = \omega/f$
10^{-1}
10^{0}
10^{1}
10^{2}
10^{3}

Fig 8c

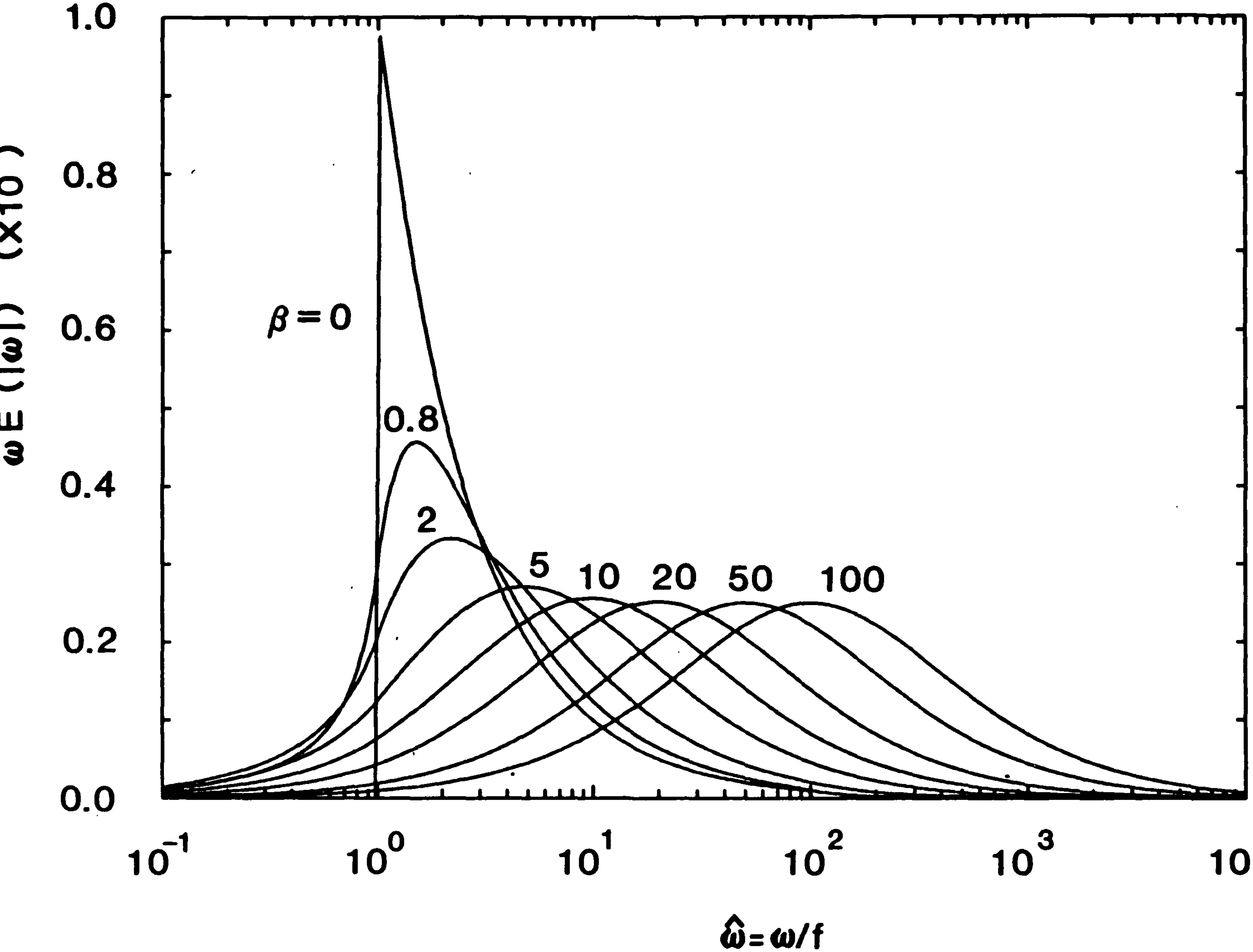

$\omega E^h(|\omega|)$ $(\times 10^4)$
1.0
0.8
0.6
0.4
0.2
0.0
$\beta = 0$
0.8
2
5
10
20
50
100
10^{-1}
10^0
10^1
10^2
10^3
10^4
$\hat{\omega} = \omega/f$

Fig. 7a

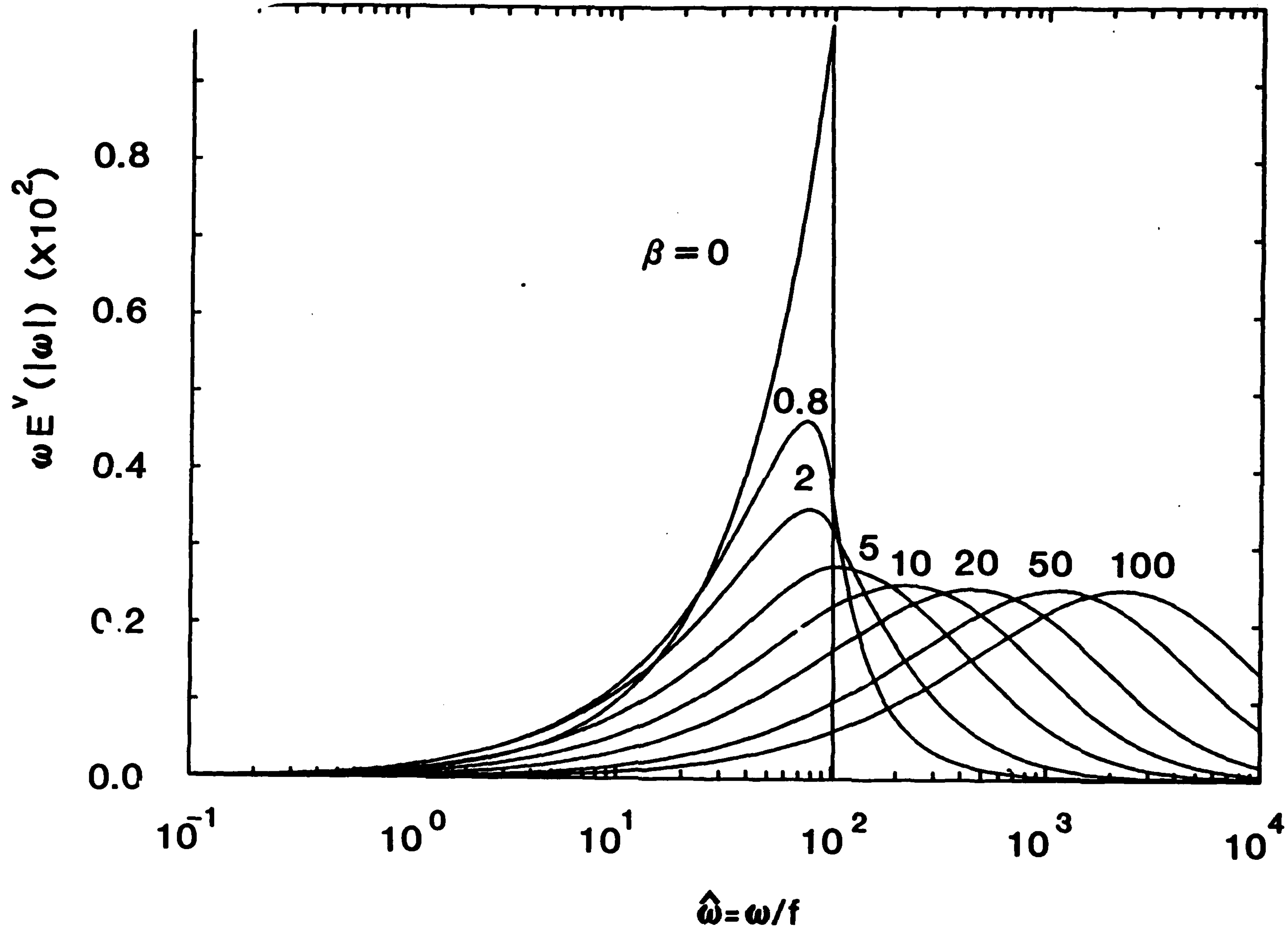
$\omega E^v(|\omega|)$ (X10^2)
0.8
0.6
0.4
0.2
0.0
$\beta = 0$
0.8
2
5
10
20
50
100
10^{-1}
10^0
10^1
10^2
10^3
10^4
$\hat{\omega} = \omega/f$

Fig. 9b

END

7-87

DTIC